Chapter

Impact Models of Gravitational and Electrostatic Forces

Klaus Wilhelm and Bhola N. Dwivedi

Abstract

The far-reaching gravitational force is described by a heuristic impact model with hypothetical massless entities propagating at the speed of light in vacuum transferring momentum and energy between massive bodies through interactions on a local basis. In the original publication in 2013, a spherical symmetric emission of secondary entities had been postulated. The potential energy problems in gravitationally and electrostatically bound two-body systems have been studied in the framework of this impact model of gravity and of a proposed impact model of the electrostatic force. These studies have indicated that an *antiparallel* emission of a secondary entity—now called *graviton*—with respect to the incoming one is more appropriate. This article is based on the latter choice and presents the modifications resulting from this change. The model has been applied to multiple interactions of gravitons in large mass conglomerations in several publications. They will be summarized here taking the modified interaction process into account. In addition, the speed of photons as a function of the gravitational potential is considered in this context together with the dependence of atomic clocks and the redshift on the gravitational potential.

Keywords: gravitation, electrostatics, potential energies, gravitational redshift and anomalies, secular mass increase

1. Introduction

Newton's law of gravity gives the attraction between two spherical symmetric bodies A and B with masses M and m, respectively, for a separation distance of their centres r (large compared to the sizes of the bodies) at rest in an inertial frame of reference. The force acting between A and B is

$$\boldsymbol{K}_{\mathrm{G}}(r) = -\frac{G_{\mathrm{N}} M \hat{\boldsymbol{r}}}{r^2}\, m, \tag{1}$$

where $G_{\mathrm{N}} = 6.674\,08(31) \times 10^{-11}\ \mathrm{m^3\ kg^{-1}\ s^{-2}}$ is the constant of gravity[1], $\hat{\boldsymbol{r}}$ is the unit vector of the radius vector $\boldsymbol{r}$ with origin at A and $r = |\boldsymbol{r}|$. The first term on the right-hand side represents the classical gravitational field of the mass M.

[1] This value and those of other constants (except h, Planck's constant, and e, charge of electron; cf. page 4 and SI, 9th edition 2019) are taken from CODATA 2014 [1].

In close analogy, Coulomb's law yields the force of the electrostatic interaction between particles C and D with charges Q and q, respectively:

$$\boldsymbol{K}_{\mathrm{E}}(r) = \frac{Q\hat{\boldsymbol{r}}}{4\pi r^2 \varepsilon_0}\, q, \tag{2}$$

where $\varepsilon_0 = 8.854\,187\,817\ldots \times 10^{-12}$ F m^{-1} is the electric constant in vacuum. Here charges with opposite signs lead to an attraction and with equal signs to a repulsion.

$$\boldsymbol{E}_Q(r) = \frac{Q\hat{\boldsymbol{r}}}{4\pi r^2 \varepsilon_0} \tag{3}$$

is the classical electrostatic field of a charge Q.

For two electrons, e.g. the ratio of the gravitational and electrostatic forces is

$$R_{\mathrm{G}}^{\mathrm{E}} = \frac{|\boldsymbol{K}_{\mathrm{E}}(r)|}{|\boldsymbol{K}_{\mathrm{G}}(r)|} = 4.16574 \times 10^{42}. \tag{4}$$

Eq. (1) yields a very good approximation of the gravitational forces, unless effects treated in the general theory of relativity (GTR) [2] are of importance.

The physical processes of the gravitational and the electrostatic fields—in particular their potential energies—are still a matter of debate: Planck [3] wondered about the energy and momentum of the electromagnetic field. A critique of the classical field theory by Wheeler and Feynman [4] concluded that a theory of action at a distance, originally proposed by Schwarzschild [5], avoids the direct notion of fields. Lange [6] calls the fact "remarkable" that the motion of a closed system in response to external forces is determined by the same law as its constituents. It should be recalled here that von Laue [7] considered radiation confined in a certain volume ("Hohlraumstrahlung") and showed that the radiation contributed to the mass of the system according to Einstein's mass-energy equation (see Eq. (51)). In a discussion of energy-momentum conservation for gravitational fields, Penrose [8] finds even for isolated systems "... something a little 'miraculous' about how things all fit together, ...", and Carlip [9] wrote in this context: "... after all, potential energy is a rather mysterious quantity to begin with ...".

Related to the potential energy problem is the disagreement of Wolf et al. and [10] and Müller et al. [11] on whether the gravitationally redshifted frequency of an atomic clock is caused by the gravitational potential

$$U(r) = -\frac{G_{\mathrm{N}} M}{r} \tag{5}$$

or by the local gravity field $\boldsymbol{g} = \nabla U$.

These remarks and disputes motivated us to think about electrostatic and gravitational fields and the problems related to the potential energies.

2. Gravitational and electrostatic interactions

If far-reaching fields have to be avoided, gravitational and electrostatic models come to mind similar to the emission of photons from a radiation source and their absorption or scattering somewhere else—thereby transferring energy and momentum with the speed of light $c_0 = 299\,792\,458$ m s^{-1} in vacuum [12–15].

We have proposed a heuristic model of Newton's law of gravitation in [16]—without far-reaching gravitational fields—involving hypothetical massless entities. Originally they had been called quadrupoles but will be called *gravitons* now. In subsequent studies, conducted to test the model hypothesis, it became evident that energy and momentum could not be conserved in a closed system without modifying the interaction process of the gravitons with massive bodies and massless particles, such as photons. The modification and the consequences in the context of the gravitational potential energy will be discussed in the following sections together with related topics.

The analogy between Newton's and Coulomb's laws suggests that in the latter case, an impact model might be appropriate as well—with electric dipole entities transferring momentum and energy. This has been proposed in [17]. The equations governing the behaviour of gravitons and dipoles in the next sections are very similar in line with the similarity of Newton's and Coulomb's laws.

Both concepts are required for a description of the gravitational redshift in terms of physical processes in Section 3.8.

2.1 Definitions of gravitons

Without a far-reaching gravitational field, the interactions have to be understood on a local basis with energy and momentum transfers by gravitons. This interpretation has several features in common with a theory based on gravitational shielding conceived by Nicolas Fatio de Duillier [18] at the end of the seventeenth century. A French manuscript can be found in [19], and an outline in German has been provided by Zehe [20]. Related ideas by Le Sage have been discussed in [21].

The gravitational case, in contrast to the electrostatic one, does not depend on polarized particles. Gravitons with an electric quadrupole configuration propagating with the speed of light c_0 will be postulated in the case of gravity. They are the obvious candidates as they have small interaction energies with positive and negative electric charges and, in addition, can easily be constructed with a spin of $S = \pm 2$, if indications to that effect are taken into account, cf. [22].

The vacuum is thought to be permeated by the gravitons that are, in the absence of near masses, isotropically distributed with (almost) no interaction among each other—even dipoles have no mean interaction energy in the classical theory (see, e.g. [23, 24]). The graviton distribution is assumed to be a nearly stable, possibly slowly varying quantity in space and time. It has a constant spatial number density:

$$\rho_{\mathrm{G}} = \frac{\Delta N_{\mathrm{G}}}{\Delta V}. \tag{6}$$

Constraints on the energy spectrum of the gravitons will be considered in later sections. At this stage we define a mean energy of

$$T_{\mathrm{G}} = |\boldsymbol{p}_{\mathbf{G}}| c_0 = p_{\mathrm{G}} c_0 \tag{7}$$

for a massless graviton with a momentum vector of $\boldsymbol{p}_{\mathbf{G}}$.

2.2 Definitions of dipoles

A model for the electrostatic force can be obtained by introducing hypothetical electric dipoles propagating with the speed of light. The force is described by the action of dipole distributions on charged particles. The dipoles are transferring momentum and energy between charges through interactions on a local basis.

Apart from the requirement that the absolute values of the positive and negative charges must be equal, nothing is known, at this stage, about the values themselves, so charges of $\pm|q|$ will be assumed, where q might or might not be identical to the elementary charge $e = 1.602176634 \times 10^{-19}$ C (exact) [25].

The electric dipole moment is

$$\pm\, \boldsymbol{d} = |q|\, \boldsymbol{l} = |q| l\, \hat{\boldsymbol{n}} \tag{8}$$

parallel or antiparallel to the velocity vector $c_0\, \hat{\boldsymbol{n}}$, where $\hat{\boldsymbol{n}}$ is a unit vector pointing in a certain direction and l is the separation distance of the charges. This assumption is necessary in order to get attraction and repulsion of charges depending on their mutual polarities. In Section 2.5 it will be shown that the value $|\boldsymbol{d}|$ of the dipole moment is not critical in the context of our model. The dipoles have a mean energy

$$T_{\mathrm{D}} = |\boldsymbol{p}_{\mathbf{D}}| c_0 = p_{\mathrm{D}} c_0, \tag{9}$$

where $\boldsymbol{p}_{\mathbf{D}}$ represents the momentum of the dipoles. As a working hypothesis, it will first be assumed that $|\boldsymbol{p}_{\mathrm{D}}|$ is constant remote from gravitational centres with the same value for all dipoles of an isotropic distribution. The dipole distribution is assumed to be nearly stable in space and time with a spatial number density

$$\rho_{\mathrm{D}} = \frac{\Delta N_{\mathrm{D}}}{\Delta V}, \tag{10}$$

but will be polarized near electric charges and affected by gravitational centres.

2.3 Virtual entities

As an important step, a formal way will be outlined of achieving the required momentum and energy transfers by discrete interactions. The idea is based on virtual gravitons and dipoles in analogy with other virtual particles, cf. [26–28].

2.3.1 Virtual gravitons

A particle with mass M is symmetrically emitting virtual gravitons with moments $\boldsymbol{p}_{\mathrm{G}}^{*}$ and energies of $T_{\mathrm{G}}^{*} \ll M c_0^2$. The emission rate is proportional to M. The gravitons will have a certain lifetime Δt_{G} and interact with "real" gravitons. In the literature, there are many different derivations of an energy-time relation, e.g. in [29–31]. Considerations of the spread of the frequencies of a limited wave-packet led Bohr [32] to an approximation for the indeterminacy of the energy that can be rewritten as

$$T_{\mathrm{G}}^{*} \approx \frac{h}{\Delta t_{\mathrm{G}}} \tag{11}$$

with $h = 6.626\,070\,15 \times 10^{-34}$ J s (exact), the Planck constant [25]. For propagating gravitons, the equation

$$T_{\mathrm{G}} = h\, \frac{c_0}{l_{\mathrm{G}}} \tag{12}$$

is equivalent to the photon energy relation $E_\nu = h\nu = h c_0/\lambda$, where λ corresponds to l_{G}, which can be considered as the wavelength of the hypothetical

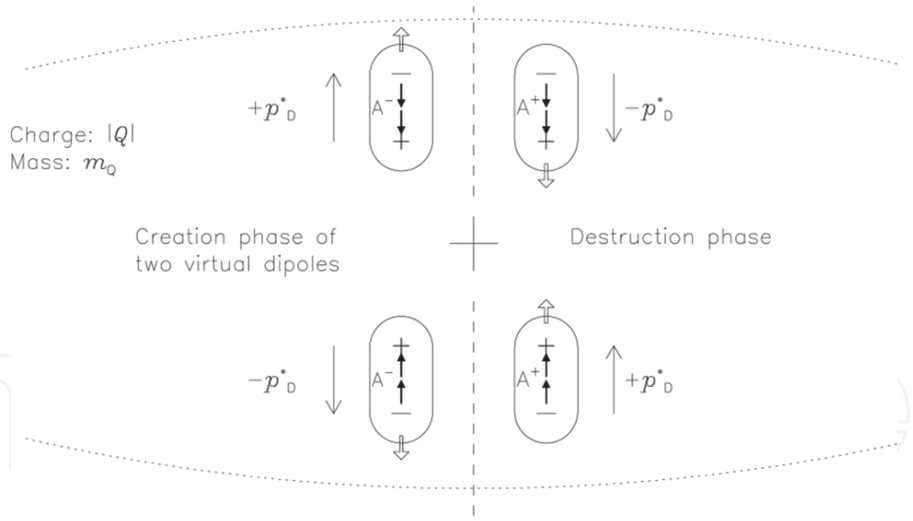

Figure 1.
Conceptional presentation of the creation and destruction phases of virtual dipole pairs by a charge and the corresponding momentum vectors of the virtual dipoles (long arrows). The dipoles are assumed to have a spin of $S = \pm 2 \times \hbar/2$ *(short arrows) (***Figure 2** *of [17]).*

gravitons. Since there is experimental evidence that virtual photons (identified as evanescent electromagnetic modes) behave non-locally [33, 34], the virtual gravitons might also behave non-locally. Consequently, the absorption of a real graviton could occur momentarily by a recombination with an appropriate virtual one.

2.3.2 Virtual dipoles

We assume that a particle with charge Q is symmetrically emitting virtual dipoles with $\boldsymbol{p}^*_{\mathrm{D}}$. The emission rate is proportional to its charge and the orientation such that a repulsion exists between the charge and the dipoles. The symmetric creation and destruction of virtual dipoles are sketched in **Figure 1**. The momentum balance is shown for the emission phase on the left and the absorption phase on the right side.

Virtual dipoles with energies of $T^*_{\mathrm{D}} \ll m_Q c_0^2$ will have a certain lifetime Δt_{D} and interact with *real* dipoles. The energy-lifetime relation

$$T^*_{\mathrm{D}} \approx \frac{h}{\Delta t_{\mathrm{D}}} \tag{13}$$

corresponds to that of the gravitons in Eq. (11). The equation

$$T_{\mathrm{D}} = h\,\frac{c_0}{l_{\mathrm{D}}} \tag{14}$$

is for propagating dipoles also equivalent to the photon energy relation, with l_{D} corresponding to λ.

2.4 Newton's law of gravity

The gravitons are absorbed by massive bodies from the background and subsequently emitted at rates determined by the mass M of the body independent of its charge:

$$\frac{\Delta N_M}{\Delta t} = \rho_{\mathrm{G}}\,\kappa_{\mathrm{G}} M = \eta_{\mathrm{G}} M, \tag{15}$$

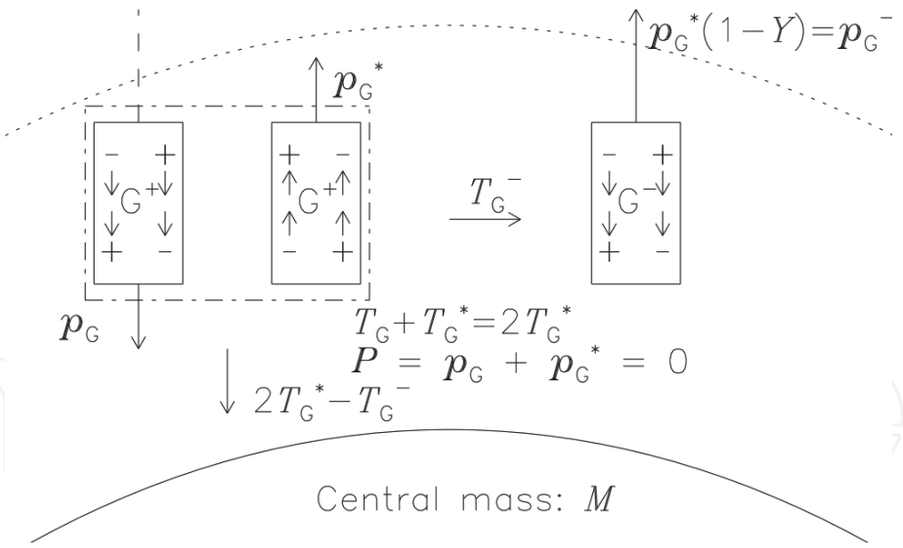

Figure 2.
Interaction of gravitons with a body of mass M. A graviton arriving with a momentum $\boldsymbol{p}_G$ on the left combines together with a virtual graviton with $\boldsymbol{p}_G^* = -\boldsymbol{p}_G$. The excess energy liberates a second virtual graviton with $\boldsymbol{p}_G^-$ on the right in a direction antiparallel to the incoming graviton. The excess energy T_G^- is smaller than T_G^*. The conceptual diagram shows gravitons with a spin $S = \pm 4 \times \hbar/2$ and G^+ or G^- orientation. It is unclear whether such a spin would have any influence on the interaction process (modified from Figure 1 of [16]).

where κ_G is the gravitational absorption coefficient and η_G the corresponding emission coefficient.

Spatially isolated particles at rest in an inertial system will be considered first. The sum of the absorption and emission rates is set equal to the intrinsic de Broglie frequency of the particle, cf. Schrödinger's Zitterbewegung [8, 35–39]. Since the absorption and emission rates must be equal in Eq. (15), this gives an emission coefficient of

$$\eta_G = \kappa_G \rho_G = \frac{1}{2}\frac{c_0^2}{h} = 6.782 \times 10^{49}\ \ \mathrm{s}^{-1}\ \ \mathrm{kg}^{-1}, \tag{16}$$

i.e. half the intrinsic de Broglie frequency, since two virtual gravitons are involved in each absorption/emission process (cf. **Figure 2**). The absorption coefficient is constant, because both ρ_G and η_G are constant. For an electron with a mass of $m_e = 9.10938356(11) \times 10^{-31}$ kg, the virtual graviton production rate equals its de Broglie frequency $\nu_{G,e}^B = m_e c_0^2/h = 1.235\ldots \times 10^{20}$ Hz.

The energy absorption rate of an atomic particle with mass M is

$$\frac{\Delta N_M}{\Delta t}\, T_G^{ab} = \kappa_G \rho_G M T_G. \tag{17}$$

Larger masses are thought of as conglomeration of atomic particles.

The emission energy, in turn, is assumed to be reduced to

$$T_G^{em} = (1 - Y)\, T_G \tag{18}$$

per graviton, where Y $(0 < Y \ll 1)$ is defined as the reduction parameter. This leads to an energy emission rate of

$$\frac{\Delta N_M}{\Delta t}\, T_G^{em} = -\eta_G M (1 - Y)\, T_G. \tag{19}$$

Without such an assumption, the attractive gravitational force could not be emulated, even with some kind of shadow effect as in Fatio's concept, cf. [18, 19].

The reduction parameter Y and its relation to the attraction are discussed below. If the energy-mass conservation [40] is applied, its consequence is that the mass of matter increases with time at the expense of the background energy of the graviton distribution.

A spherically symmetric emission of the liberated gravitons had been assumed in [16]. Further studies summarized in Sections 3.1, 3.6 and 3.8 indicated that an *antiparallel* emission with respect to the incoming graviton has to be assumed in order to avoid conflicts with energy and momentum conservation principles in closed systems. This important assumption can best be explained by referring to **Figure 2**. The interaction is based on the combination of a virtual graviton with momentum $\boldsymbol{p}_{\mathrm{G}}^{*}$ and an incoming graviton with $\boldsymbol{p}_{\mathrm{G}}$ followed by the liberation of another virtual graviton in the opposite direction supplied with the excess energy T_{G}^{-}. Regardless of the processes operating in the immediate environment of a massive body, it must attract the mass of the combined real and virtual gravitons, which will be at rest in the reference frame of the body. The excess energy T_{G}^{-} is, therefore, reduced and so will be the liberation energy, as assumed in Eq. (18). The emission in Eq. (19) will give rise to a flux of gravitons with reduced energies in the environment of a body with mass M. Its spatial density is

$$\rho_M(r) = \frac{\Delta N_M}{\Delta V_r} = \frac{\Delta N_M}{\Delta t}\frac{1}{4\pi r^2 c_0} = \eta_{\mathrm{G}}\frac{M}{4\pi r^2 c_0}, \tag{20}$$

where the volume increase in the time interval Δt is

$$\Delta V_r = 4\pi r^2 c_0\,\Delta t. \tag{21}$$

The radial emission is part of the background in Eq. (6), which has a larger number density ρ_{G} than $\rho_M(r)$ at most distances r of interest. Note that the emission of the gravitons from M does not change the number density or the total number of gravitons. For a certain r_M, defined as the mass radius of M, it has to be

$$\rho_{\mathrm{G}} = \left[\frac{\Delta N_M}{\Delta V_r}\right]_{r_M} = \frac{\eta_{\mathrm{G}}}{c_0}\frac{M}{4\pi r_M^2}, \tag{22}$$

because all gravitons of the background that come so close interact with the mass M in some way. The same arguments apply to a mass $m \neq M$ and, in particular, to the electron mass m_{e}.

Therefore

$$\sigma_{\mathrm{G}} = \frac{m}{4\pi r_m^2} = \frac{M}{4\pi r_M^2} = \frac{m_{\mathrm{e}}}{4\pi r_{\mathrm{G,e}}^2} \tag{23}$$

will be independent of the mass as long as the density of the background distribution is constant. The quantity σ_{G} is a kind of surface mass density. The equation shows that σ_{G} is determined by the electron mass radius $r_{\mathrm{G,e}}$, for which estimates will be provided in Sections 3.2 and 3.3. From Eqs. (16), (22) and (23), it follows that

$$\kappa_{\mathrm{G}}\sigma_{\mathrm{G}} = c_0. \tag{24}$$

The flux of modified gravitons from M will interact with a particle of mass m and vice versa. The interaction rate in the static case can be found in Eqs. (15) and (20):

$$\frac{\Delta N_{M,m}(r)}{\Delta t} = \kappa_G m \frac{\Delta N_M}{\Delta V_r} = \frac{\kappa_G \eta_G}{c_0} \frac{Mm}{4\pi r^2} = \frac{\kappa_G c_0}{2h} \frac{mM}{4\pi r^2} = \kappa_G M \frac{\Delta N_m}{\Delta V_r} = \frac{\Delta N_{m,M}(r)}{\Delta t}. \quad (25)$$

A calculation with *antiparallel* emissions of the secondary gravitons shows that an interaction of a graviton with reduced momentum $\boldsymbol{p}_G^-$ provides $-\boldsymbol{p}_G\left(2Y - Y^2\right)$ together with its unmodified counterpart from the opposite sides. The resulting imbalance will be

$$\frac{\Delta \boldsymbol{P}_{M,m}(r)}{\Delta t} \approx -2\,\boldsymbol{p}_G Y \frac{\Delta N_{M,m}(r)}{\Delta t} = -\boldsymbol{p}_G Y \kappa_G \frac{c_0}{h} \frac{Mm}{4\pi r^2}, \quad (26)$$

if the quadratic terms in Y can be neglected for very small Y scenarios.

The imbalance will cause an attractive force that is responsible for the gravitational pull between bodies with masses M and m. By comparing the force expression in Eq. (26) with Newton's law in Eq. (1), a relation between p_G, Y, κ_G and G_N can be established through the constant G_G:

$$G_G = p_G Y \kappa_G \approx 4\pi G_N \frac{h}{c_0} = 1.853\ldots \times 10^{-51}\ \mathrm{m^4\ s^{-2}}. \quad (27)$$

It can be seen that Y does not depend on the mass of a body. Since Eq. (18) allows stable processes over cosmological time scales only, if Y is very small, we assume in **Figure 3** that $Y < 10^{-15}$.

Note that the mass of a body and thus its intrinsic de Broglie frequency are not strictly constant in time, although the effect is only relevant for cosmological time scales (see lower panel of **Figure 3**). In addition, multiple interactions will occur within large mass conglomerations (see Sections 3.4–3.6) and can lead to deviations from Eqs. (1).

The graviton energy density remote from any masses will be

$$\epsilon_G = T_G \rho_G = \frac{2\pi G_N}{Y} \sigma_G^2, \quad (28)$$

where the last term is obtained from Eq. (27) with the help of Eqs. (16) and (22)–(24).

What will be the consequences of the mass accretion required by the modified model? With Eqs. (17), (19) and (27), it follows that the relative mass accretion rate of a particle with mass M will be

$$A = \frac{1}{M} \frac{\Delta M}{\Delta t} = \frac{2\pi G_N}{c_0} \sigma_G = \frac{2\pi G_N}{c_0} \frac{m_e}{4\pi r_{G,e}^2}, \quad (29)$$

which implies an exponential growth according to

$$M(t) = M_0 \exp\left[A\,(t - t_0)\right] \approx M_0\,(1 + A\,\Delta t), \quad (30)$$

where $M_0 = M(t_0)$ is the initial value at t_0 and the linear approximation is valid for small $A\,(t - t_0) = A\,\Delta t$. The accretion rate is

$$A = \frac{1.014 \times 10^{-49}}{r_{G,e}^2}\ \ \mathrm{m^2\ \ s^{-1}}, \quad (31)$$

if the expression is evaluated in terms of recent parameters.

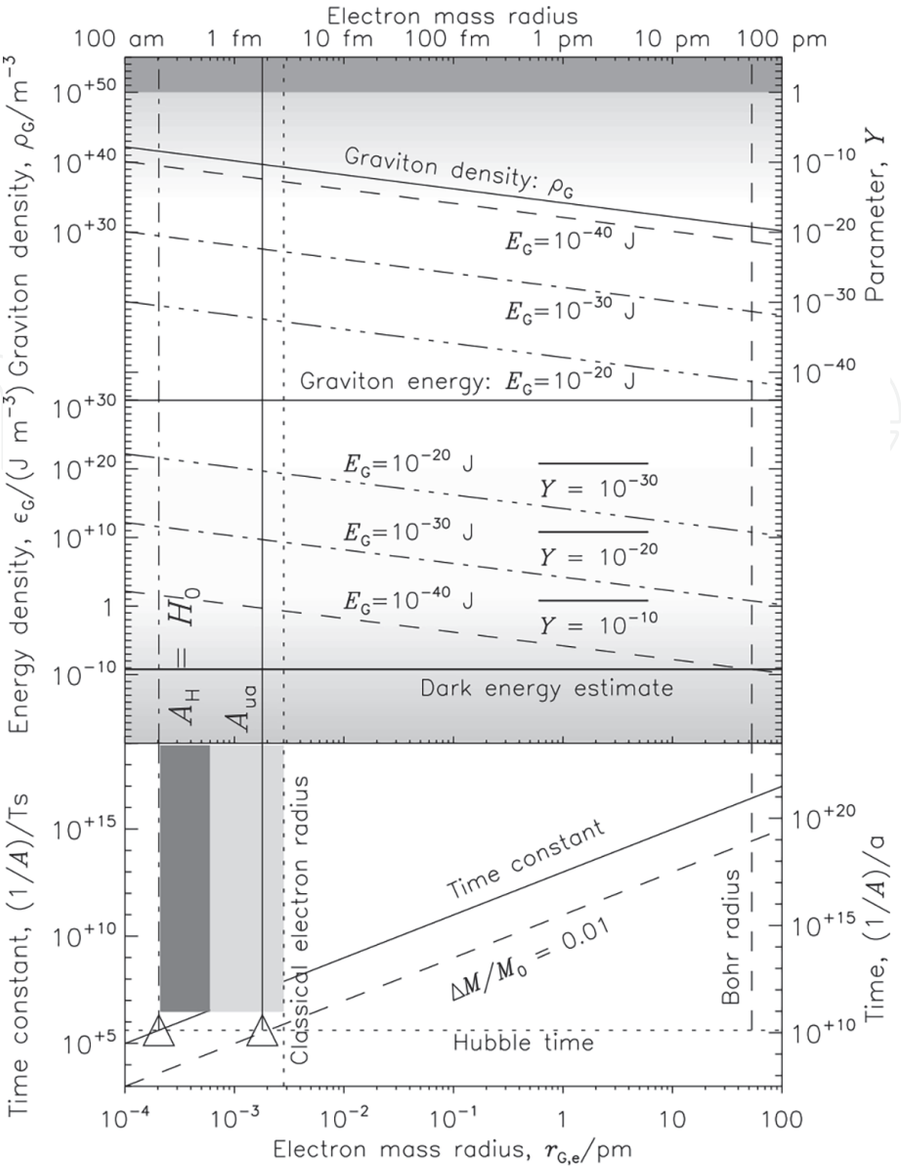

Figure 3.
Energies of $E_G = (10^{-40}$ to $10^{-20})$ J are assumed for the gravitons, as indicated in the upper and middle panels by different line styles. In the upper panel, the spatial number density of gravitons and the corresponding reduction parameter Y of Eq. (18) are plotted as functions of the electron mass radius $r_{G,e}$. The range $Y \geq 1$ (dark shading) is obviously completely excluded by the model. Even values greater than $\approx 10^{-15}$ are not realistic (light shaded region), cf. paragraph following Eq. (27). The cosmic dark energy estimate (3.9 ± 0.4) GeV m^{-3} $= (6.2 \pm 0.6) \times 10^{-10}$ J m^{-3} (see [44]) is marked in the second panel. It is well below the acceptable range (light shaded and unshaded regions in the middle panel). If, however, only the Y portion is taken into account in the dark energy estimate, the total energy density could be many orders of magnitude larger as shown for Y from 10^{-10} to 10^{-30} by short horizontal bars. In the lower panel, the mass accretion time constant and the time required for a relative mass increase of 1% are shown (on the right side in units of years). Indicated is also the Hubble time $1/H_0$ as well as the lower limit of the electron mass radius (left triangle and dark shaded area) estimated from the Pioneer anomaly. The light shaded area takes smaller Pioneer anomalies into account (see Section 3.2). It is shown up to the vertical dotted line for the classical electron radius of 2.82 fm. The right triangle and the vertical solid line show the result in Section 3.3 based on the observed secular increase of the Sun-Earth distance [45] (modified from **Figure 2** *of [16]).*

The gravitational quantities are displayed with these assumptions in a wide parameter range in **Figure 3** (although the limits are set rather arbitrarily). The lower panel displays the time constant of the mass accretion. It indicates that a significant mass increase would be expected within the standard age of the Universe of the order of $1/H_0$ (with the Hubble constant H_0) only for very small $r_{G,e}$.

Fahr and Heyl [41] have suggested that a decay of the vacuum energy density creates mass in an expanding universe, and Fahr and Siewert [42] found a mass creation rate in accordance with Eq. (30).

The relative uncertainty of the present knowledge of the Rydberg constant

$$R_\infty = \frac{\alpha^2 m_e c_0}{2h} = 10\,973\,731.568\,508\ \ \mathrm{m}^{-1} \tag{32}$$

is $u_r \approx 5.9 \times 10^{-12}$, where

$$\alpha = \frac{e^2}{2\varepsilon_0 c_0 h} = 7.297\,352\,5664(17) \times 10^{-3} \tag{33}$$

is Sommerfeld's fine-structure constant. Since spectroscopic observations of the distant universe with redshifts up to $z \leq 0.5$ are compatible with modern data, it appears to be reasonable to set $(1+u_r)M_0 \geq M(t) > M_0$ at least for the time interval $\Delta t \leq 1.6 \times 10^{17}$ s. Any variation of R_∞, caused by the linear dependence upon the electron mass, which has also been considered in [43], would then be below the detection limit for state-of-the-art methods.

From the emission rate and the lifetime of virtual gravitons in Eqs. (15) and (11), an estimate of their total number and energy at any time can thus be obtained for a body with mass M as

$$N_G^{tot} = \Delta t_G \frac{Mc_0^2}{h} \tag{34}$$

and

$$T_G^{tot} = N_G^{tot} T_G^* \approx Mc_0^2, \tag{35}$$

i.e. the mass of a particle would reside within the virtual gravitons.

2.5 Coulomb's law

2.5.1 Electrostatic fields and charged particles

Coulomb's law in Eq. (2) gives the attractive or repulsive electrostatic force between two charged particles at rest in an inertial system. Together with the electrostatic field in Eq. (3), it can be written as

$$\boldsymbol{K}_E(r) = \boldsymbol{E}_Q(r) q. \tag{36}$$

The electrostatic potential $U_E(r)$ of a charge Q, located at $r = 0$, is for $r > 0$

$$U_E(r) = \frac{Q}{4\pi r \varepsilon_0}. \tag{37}$$

The corresponding electrostatic field can thus be written as $\boldsymbol{E}_Q(r) = -\nabla U_E(r)$.

2.5.2 Dipole interactions

Note that the dipoles in the background distribution, cf. Eq. (10), have no mean interaction energy, even in the classical theory (see, e.g. [24]). Whether this

"background dipole radiation" and the "graviton radiation" are related to the dark matter (DM) and dark energy (DE) problems is of no concern here but could be an interesting speculation.

A charge Q absorbs and emits dipoles at a rate

$$\frac{\Delta N_Q}{\Delta t} = \kappa_D \rho_D |Q| = \eta_D |Q|, \tag{38}$$

where η_D and κ_D are the corresponding (dipole) emission and absorption coefficients.

From energy conservation it follows that absorption and emission rates of dipoles in Eq. (38) of a body with charge Q must be equal. The momentum conservation can, in general, be fulfilled by isotropic absorption and emission processes.

The interaction processes assumed between a positively charged body and dipoles is sketched in **Figure 4**. A mass m_Q of the charge Q has explicitly been mentioned, because the massless dipole charges are not assumed to absorb and emit any dipoles themselves. The conservation of momentum could hardly be fulfilled in such a process. In Section 3.8 we postulate, however, that gravitons interact with dipoles and thereby control their momentum and speed, subject to the condition that $p_G \ll p_D$.

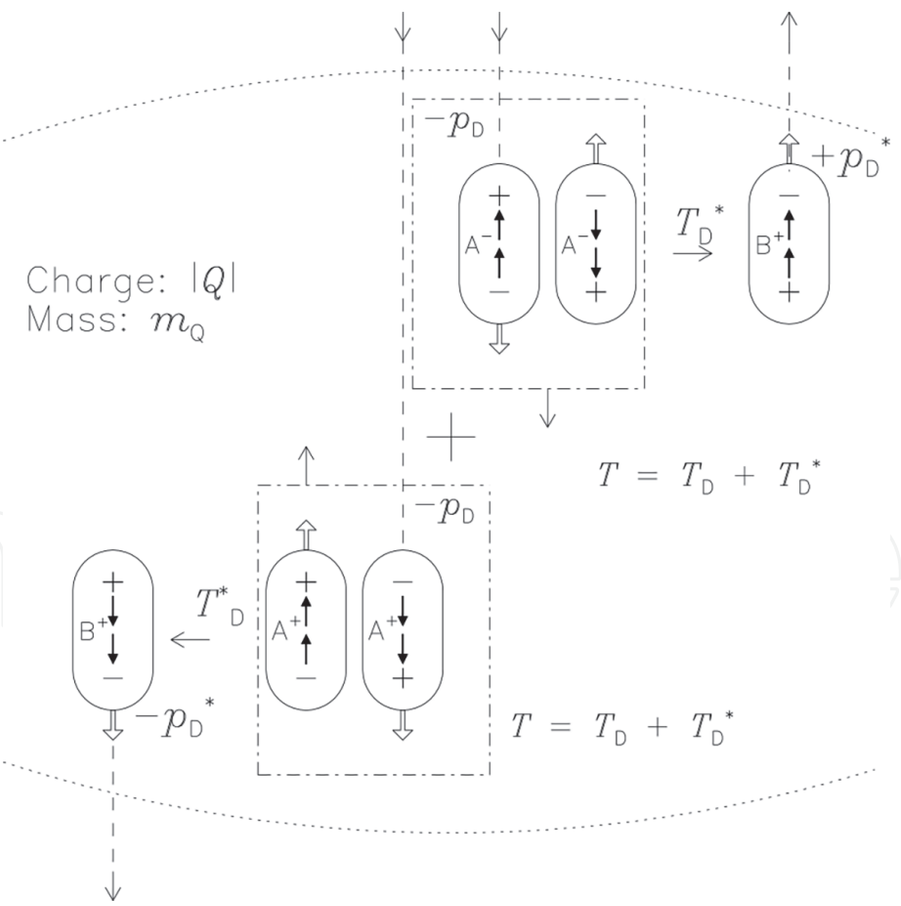

Figure 4.
Virtual dipoles emitted by a charge +|Q| (with mass m_Q) interact with real dipoles, A^+ and A^- arriving with a momentum $-\boldsymbol{p}_D$, each. On the left, a dipole A^+ combines in the lower dashed-dotted box with virtual dipole A^+ in its destruction phase and liberates dipole B^+. No momentum will be transferred to the central charge with $p_D = p_D^*$. The other types of interaction—called direct interaction, in contrast to the indirect one on the left—also require two virtual dipoles, one of them combines in its creation phase with dipole A^- (in the upper box with dashed-dotted boundaries), and the other one is liberated by the excess energy of the annihilation. The central charge received a momentum of $-(p_D + p_D^*) = -2p_D$. No spin reversal has been assumed in both cases.

The assumptions as outlined will lead to a distribution of the emitted dipoles in the rest frame of an isolated charge Q with a spatial density of

$$\rho_{\mathrm{Q}}(r) = \frac{\Delta N_Q}{\Delta V_r} = \frac{1}{4\pi r^2 c_0}\frac{\Delta N_Q}{\Delta t} = \eta_{\mathrm{D}}\frac{|Q|}{4\pi r^2 c_0}, \tag{39}$$

where ΔV_r is given in Eq. (21). The radial emission is part of the background ρ_{D}, which has a larger number density than $\rho_D(r)$ at most distances r of interest. Note that the emission of the dipoles from Q does not change the number density ρ_{D} in the environment of the charge but reverses the orientation of *half* of the dipoles affected.

The total number of dipoles will, of course, not be changed either. For a certain r_Q, defined as the charge radius of Q, it has to be

$$\rho_{\mathrm{D}} = \left[\frac{\Delta N_Q}{\Delta V_r}\right]_{r_Q} = \frac{\eta_{\mathrm{D}}}{c_0}\frac{|Q|}{4\pi r_{\mathrm{Q}}^2}, \tag{40}$$

because all dipoles of the background that come so close interact with the charge Q in some way. The same arguments apply to a charge $q \neq Q$. Since ρ_{D} cannot depend on either q or Q, the quantity

$$\sigma_{\mathrm{Q}} = \frac{|Q|}{4\pi r_{\mathrm{Q}}^2} = \frac{|q|}{4\pi r_q^2} = \frac{|e|}{4\pi r_e^2} \tag{41}$$

must be independent of the charge and can be considered as a kind of surface charge density, cf. "Flächenladung" of an electron defined by Abraham [46], which is the same for all charged particles. The equation shows that σ_Q is determined by the electron charge radius r_e.

At this stage, this is a formal description awaiting further quantum electrodynamic studies in the near-field region of charges. It might, however, be instructive to provide a speculation for the dipole emission rate $\Delta N_Q/\Delta t$ of a charge Q. The physical constants α, c_0, h, ϵ_0 and G_{N} can be combined to give a dipole emission coefficient

$$\eta_{\mathrm{D}} = \frac{1}{2}\frac{\alpha^2 c_0^2}{h\sqrt{\epsilon_0 G_{\mathrm{N}}}} = 1.486 \times 10^{56}\ \ \mathrm{s}^{-1}\ \ \mathrm{C}^{-1} \tag{42}$$

as half the virtual dipole production rate and thus for a charge $|e|$ a rate of

$$\frac{\Delta N_e}{\Delta t} = \eta_{\mathrm{D}}|e| = 2.380 \times 10^{37}\ \ \mathrm{s}^{-1}. \tag{43}$$

Note that the dipole emission rate is fixed for a certain charge and does not depend on the particle mass. From Eqs. (38), (40) and (41), we get

$$\kappa_{\mathrm{D}}\sigma_Q = c_0. \tag{44}$$

During a *direct* interaction, the dipole A^- (arriving in **Figure 4** from above on the right side) combines together with an identical virtual dipole with an opposite velocity vector. This postulate is motivated by the fact that it provides the easiest way to eliminate the charges and yield $P = -p_{\mathrm{D}} + p_{\mathrm{D}}^* = 0$, where $p_{\mathrm{D}}^* = p_{\mathrm{D}}$ is the magnitude of the momentum vector of a virtual dipole, cf. Eq. (9). The momentum balance is neutral, and the excess energy T_{D} is used to liberate a second virtual

dipole B^+, which has the required orientation. The charge had emitted two virtual dipoles with a momentum of $+p_D^*$, each, and a total momentum of $-(p_D + p_D^*) = -2p_D$ was transferred to $|Q|$. The process can be described as a reflection of a dipole together with a reversal of the dipole momentum. The number of these direct interactions will be denoted by $\Delta\hat{N}_Q$. The dipole of type A^+ (arriving from above on the left side) can exchange its momentum in an *indirect* interaction only on the far side of the charge with an identical virtual dipole during its absorption (or destruction) phase (cf. **Figure 1**). The excess energy of T_D is supplied to liberate a second virtual dipole B^+. The momentum transfer to the charge $+|Q|$ is zero. This process just corresponds to a double charge exchange. Designating the number of interactions of the indirect type with $\Delta\tilde{N}_Q$, it is

$$\frac{\Delta N_Q}{\Delta t} = \frac{\Delta\hat{N}_Q + \Delta\tilde{N}_Q}{\Delta t} \tag{45}$$

with $\Delta\tilde{N}_Q = \Delta\hat{N}_Q = \Delta N_Q/2$. Unless direct and indirect interactions are explicitly specified, both types are meant by the term "interaction". The virtual dipole emission rate in **Figure 4** has to be

$$\frac{\Delta N_Q^*}{\Delta t} = 2\,\frac{\Delta N_Q}{\Delta t}, \tag{46}$$

i.e. the virtual dipole emission rate equals the sum of the real absorption and emission rates. The interaction model described results in a mean momentum transfer per interaction of p_D *without involving a macroscopic electrostatic field*.

A quantitative evaluation gives the force acting on a test particle with charge q at a distance r from another particle with charge Q. This results from the absorption of dipoles not only from the background but also from the distribution emitted from Q according to Eq. (39) under the assumption of a *constant* absorption coefficient κ_D in Eq. (38). The rate of interchanges between these charges then is

$$\frac{\Delta N_{Q,q}(r)}{\Delta t} = \kappa_D\,|q|\,\frac{\Delta N_Q}{\Delta V_r} = \frac{\kappa_D\,\eta_D}{c_0}\,\frac{|Q|\,|q|}{4\pi r^2} = \kappa_D\,|Q|\,\frac{\Delta N_q}{\Delta V_r} = \frac{\Delta N_{q,Q}(r)}{\Delta t}, \tag{47}$$

which confirms the reciprocal relationship between q and Q. The equation, also very similar to Eq. (25), does not contain an explicit value for η_D. It is important to realize that all interchange events between pairs of charged particles are either direct or indirect depending on their polarities and transfer of a momentum of $\pm 2p_D$ or zero.

The external electrostatic potential of a spherically symmetric body C with charge Q is given in Eq. (37). Since the electrostatic force between the charged particles C and D is typically many orders of magnitude larger than the gravitational force, we only take the electrostatic effects into account in this section and neglect the gravitational interactions.

In order to have a well-defined configuration for our discussion, we will assume that body C with mass m_C has a positive charge $Q > 0$ and is positioned at a distance r beneath body D (mass m_D) with either a charge $+|q|$ in **Figure 5** or $-|q|$ in **Figure 6**. Only the processes near body D are shown in detail.

The interaction rates of dipoles with bodies C and D in Eq. (47) (the same for both bodies even if $|Q| \neq |q|$) and the momentum transfers indicated in **Figures 5** and **6**, respectively, lead to a norm of the momentum change rate for bodies C and D of

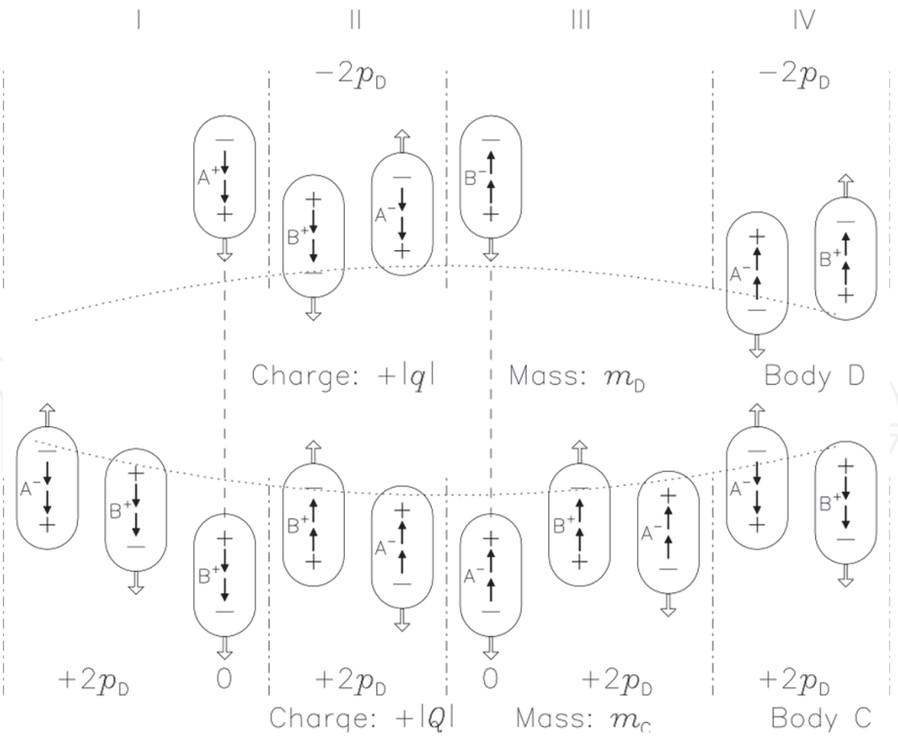

Figure 5.
Body C with charge $Q > 0$ and mass m_C is positioned in this configuration beneath body D with charge $+|q|$ and mass m_D leading to an electrostatic repulsion of the bodies. This results from the reversal of dipoles by the charge Q followed by direct interactions with the charge $+|q|$ as defined on the right-hand side of **Figure 4**. *Two reversals are schematically indicated in columns I and III. The dipoles arriving in columns II and IV from below have the same polarity as if they would be part of the background distribution and do not contribute to the momentum transfer, because of a compensation by dipoles arriving from above. The net momentum transfer caused by the two interacting reversed dipoles thus is $4\boldsymbol{p}_D$, i.e. $2\boldsymbol{p}_D$ per dipole (modified from* **Figure 3** *of [17]).*

$$\left|\frac{\Delta \boldsymbol{P}_{\mathrm{Q,q}}(r)}{\Delta t}\right| = 2p_{\mathrm{D}}\,\frac{\Delta N_{\mathrm{Q,q}}(r)}{\Delta t} = 2p_{\mathrm{D}}\,\frac{\kappa_{\mathrm{D}}\,\eta_{\mathrm{D}}}{c_0}\,\frac{Q\,|q|}{4\pi r^2}. \tag{48}$$

Together with

$$p_{\mathrm{D}}\,\frac{\kappa_{\mathrm{D}}\,\eta_{\mathrm{D}}}{c_0} = \frac{T_{\mathrm{D}}\,\kappa_{\mathrm{D}}\,\eta_{\mathrm{D}}}{c_0^2} = \frac{1}{2\varepsilon_0} \tag{49}$$

this leads, depending on the signs of the charges Q and q, to a repulsive or an attractive electrostatic force between C and D in accordance with Coulomb's law in Eq. (2).

Important questions are related to the energy T_{D} and momentum $\boldsymbol{p}_{\mathrm{D}}$ of the dipoles and, even more, to their energy density in space. Eqs. (9), (40), (41) and (44) together with Eq. (49) allow the energy density to be expressed by

$$\epsilon_{\mathrm{D}} = T_{\mathrm{D}}\,\rho_{\mathrm{D}} = \frac{\sigma_{\mathrm{D}}^2}{2\varepsilon_0}. \tag{50}$$

This quantity is independent of the dipole energy. It takes into account all dipoles (whether their distribution is chaotic or not). Should the energy density vary in space and/or time, the surface charge density σ_Q must vary as well.

If we assume that the electron charge radius r_Q in Eq. (41) equals the classical electron radius $r_{\mathrm{e}} = 2.82$ fm, then an energy density of $\epsilon_{\mathrm{D}} = 1.45 \times 10^{29}$ J m^{-3} (very high compared to the present cosmic dark energy estimate) follows from

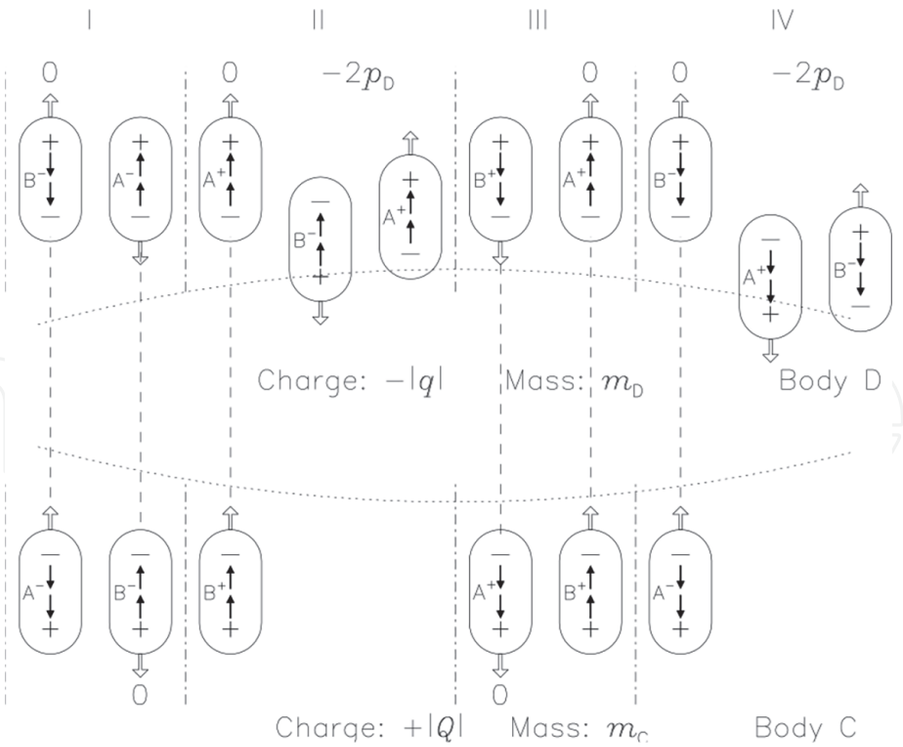

Figure 6.
Body C is again positioned beneath body D. The charge of D is now $-|q|$, however, leading to an electrostatic attraction of the bodies. The attraction results from the reversal of dipoles by the charge $Q > 0$ followed by indirect interactions with charge $-|q|$ as defined on the left-hand side of ***Figure 4****. Two events without momentum transfer are schematically indicated in columns II and IV. The dipoles arriving in columns I and III from below have the same polarity as if they would be part of the background distribution. The same is true for all dipoles arriving from above. The net momentum transfer caused by the two reversed dipoles thus is $-4\boldsymbol{p}_D$, i.e. $-2\boldsymbol{p}_D$ per dipole (modified from* **Figure 4** *of [17]).*

Eq. (50). The dipole density $\rho_D = 7.95 \times 10^{56}\ \mathrm{m}^{-3}$ in Eq. (40) is also very high, leading to a dipole energy of $T_D = 1.83 \times 10^{-28}$ J. If, on the other hand, we identify the dipole distribution with DM with an estimated energy density of $2.48 \times 10^{-10}\ \mathrm{J\ m}^{-3}$ and require that the dipole energy density corresponds to this value, then extreme values follow for $r_Q = 13.9\,\mu\mathrm{m}$, $\rho_D = 3.28 \times 10^{37}\ \mathrm{m}^{-3}$ and $T_D = 7.55 \times 10^{-48}$ J.

3. Applications of impact models

The detection of gravitons and dipoles with the expected properties would, of course, be the best verification of the proposed models. Lacking this, indirect support can be found through the application of the models with a view to describe physical processes successfully for specific situations.

3.1 Potential energies

3.1.1 Gravitational potential energy

As mentioned in Section 1, the study of the potential energy problem [47] had been motivated by the remark that the potential energy is rather mysterious [9].[2]

[2] In this context, it is of interest that Brillouin [48] discussed this problem in relation to the electrostatic potential energy.

It led to the identification of the "source region" of the potential energy for the special case of a system with two masses M_E and M_M subject to the condition $M_E \gg M_M$. An attempt to generalize the study without this condition required either violations of the energy conservation principle as formulated by von Laue [49] for a closed system or a reconsideration of an assumption we made concerning the gravitational interaction process in [16]. The change necessary to comply with the energy conservation principle has been discussed in Section 2.4. A generalization of the potential energy concept for a system of two spherically symmetric bodies A and B with masses m_A and m_B without the above condition could then be formulated [50].

We will again exclude any further energy contributions, such as rotational or thermal energies, and make use of the fact that the external gravitational potential of a spherically symmetric body of mass M and radius $\boldsymbol{r}$ in Eq. (5) is that of a corresponding point mass at the centre.

The energy E_m and the momentum $\boldsymbol{p}$ of a free particle with mass m moving with a velocity $\boldsymbol{v}$ relative to an inertial reference system are related by

$$E_m^2 - \boldsymbol{p}^2 c_0^2 = m^2 c_0^4, \tag{51}$$

where $\boldsymbol{p}$ is the momentum vector

$$\boldsymbol{p} = \boldsymbol{v}\,\frac{E_m}{c_0^2} \tag{52}$$

[40, 51]. For an entity in vacuum with no rest mass ($m = 0$), such as a photon [15, 52, 53], the energy-momentum relation in Eq. (51) reduces to

$$E_\nu = p_\nu c_0. \tag{53}$$

In [50] we assume that two spherically symmetric bodies A and B with masses m_A and m_B, respectively, are placed in space remote from other gravitational centres at a distance of $r + \Delta r$ reckoned from the position of A. Initially both bodies are at rest with respect to an inertial reference frame represented by the centre of gravity of both bodies. The total energy of the system then is with Eq. (51) for the rest energies and with Eq. (5) for the potential energy

$$E_S = (m_A + m_B)c_0^2 - G_N\,\frac{m_A m_B}{r + \Delta r}. \tag{54}$$

The evolution of the system during the approach of A and B from $r + \Delta r$ to r can be described in classical mechanics. According to Eq. (48), the attractive force between the bodies during the approach is approximately constant for $r \gg \Delta r > 0$, resulting in accelerations of $b_A = |K_G(r)|/m_A$ and $b_B = -|K_G(r)|/m_B$, respectively. Since the duration Δt of the free fall of both bodies is the same, the approach of A and B can be formulated as

$$\Delta r = s_A - s_B = \frac{1}{2}\,(b_A - b_B)\,(\Delta t)^2 = \frac{1}{2}\left(\frac{1}{m_A} + \frac{1}{m_B}\right)\,|K_G(r)|\,(\Delta t)^2, \tag{55}$$

showing that $s_A m_A = -s_B m_B$, i.e. the centre of gravity stays at rest. Multiplication of Eq. (55) by $|K_G(r)|$ gives the corresponding kinetic energy equation

$$|K_G(r)|\,\Delta r = \frac{1}{2}\left(\frac{K_G^2(r)\,(\Delta t)^2}{m_A} + \frac{K_G^2(r)\,(\Delta t)^2}{m_B}\right) = \frac{1}{2}\,m_A v_A^2 + \frac{1}{2}\,m_B v_B^2 = T_A + T_B. \tag{56}$$

The kinetic energies[3] T_A and T_B should, of course, be the difference of the potential energy term in Eq. (54) at distances of r and $r + \Delta r$. We find indeed for small Δr with Newton's law in Eq. (1):

$$G_N m_A m_B \left(\frac{1}{r} - \frac{1}{r+\Delta r}\right) \approx G_N \frac{m_A m_B}{r^2} \Delta r = |K_G(r)| \Delta r. \tag{57}$$

We may now ask the question, whether the impact model can provide an answer to the potential energy "mystery" in a closed system. Since the model implies a secular increase of mass of all bodies, it obviously violates a closed-system assumption. The increase is, however, only significant over cosmological time scales, and we can neglect its consequences in this context. A free single body will, therefore, still be considered as a closed system with constant mass. In a two-body system, both masses m_A and m_B will be constant in such an approximation, but now there are gravitons interacting with both masses.

The number of gravitons travelling at any instant of time from one mass to the other can be calculated from the interaction rate in Eq. (25) multiplied by the travel time r/c_0:

$$\Delta N_{m_A,m_B}(r) = \frac{\kappa_G}{8\pi h} \frac{m_A m_B}{r}. \tag{58}$$

The same number is moving in the opposite direction. The energy deficiency of the interacting gravitons with respect to the corresponding background then is together with Eqs. (18) and (27) for each body

$$\Delta E_G(r) = -p_G Y \kappa_G \frac{c_0}{8\pi h} \frac{m_A m_B}{r} = -G_G \frac{c_0}{8\pi h} \frac{m_A m_B}{r} = -\frac{G_N}{2} \frac{m_A m_B}{r}. \tag{59}$$

The last term shows—with reference to Eq. (57)—that the energy deficiency ΔE_G equals *half* the potential energy of body A at a distance r from body B and vice versa.

We now apply Eq. (59) and calculate the difference of the energy deficiencies for separations of $r + \Delta r$ and r for interacting gravitons travelling in both directions and get

$$2\{\Delta E_G(r+\Delta r) - \Delta E_G(r)\} = G_N m_A m_B \left(\frac{1}{r} - \frac{1}{r+\Delta r}\right). \tag{60}$$

Consequently, the difference of the potential energies between $r + \Delta r$ and r in Eq. (57) is balanced by the difference of the total energy deficiencies.

The physical processes involved can be described as follows:

1. The number of gravitons on their way for a separation of $r + \Delta r$ is smaller than that for r, because the interaction rate depends on r^{-2} according to Eq. (48), whereas the travel time is proportional to r.

2. A decrease of $r + \Delta r$ to r during the approach of A and B increases the number of gravitons with reduced energy.

---

[3] Eqs. (51) and (52) together with $E_0 = mc_0^2$ [c] and $\gamma = 1/\sqrt{1 - v^2/c_0^2}$ yield the relativistic kinetic energy of a massive body: $T = E - E_0 = E_0(\gamma - 1)$. The evaluations for T_A and T_B agree in very good approximation with Eq. (56) for small v_A and v_B.

3. The energies liberated by energy reductions are available as potential energy and are converted into kinetic energies of bodies A and B.

4. With Eqs. (51) and (52) and the approximations in Footnote 3, it follows that the sum of the kinetic energies T_A and T_B, the masses A and B, plus the total energy deficiencies of the interacting gravitons can indeed be considered to be a closed system as defined by von Laue [49].

3.1.2 Electrostatic potential energy.

In this section we will discuss the electrostatic aspects of the potential energy. The energy density of an electrostatic field $\boldsymbol{E}$ outside of charges is given by

$$w = \frac{\varepsilon_0}{2}\,\boldsymbol{E}^2, \tag{61}$$

cf., e.g. [24, 54]. Applying Eq. (61) to a plane-plate capacitor with an area F, a plate separation b and charges $\pm|Q|$ on the plates, the energy stored in the field of the capacitor turns out to be

$$W = \frac{\varepsilon_0}{2}\,\boldsymbol{E}^2 F b = \frac{\varepsilon_0}{2}\boldsymbol{E}^2 V. \tag{62}$$

With a potential difference $\Delta U_E = |\boldsymbol{E}|b$ and a charge of $Q = \varepsilon_0|\boldsymbol{E}|F$ (increased incrementally to these values), the potential energy of Q at ΔU_E is

$$W = \frac{1}{2}\,Q\,\Delta U_E. \tag{63}$$

The question as to where the energy is actually stored, [54] answered by showing that both concepts implied by Eqs. (62) and (63) are equivalent.

Can the impact model provide an answer for the electrostatic potential energy in a closed system, where dipoles are interacting with two charged bodies? This question we posed in [55]: the number of reversed dipoles travelling at any instant of time from a charge $Q > 0$ to q in **Figures 5** and **6** can be calculated from the interaction rate in Eq. (47) multiplied by a travel time $\Delta t = r/c_0$:

$$\Delta N_{Q,q}(r) = \frac{\kappa_D \eta_D}{c_0^2}\,\frac{Q\,|q|}{4\pi r}. \tag{64}$$

The same number of dipoles is moving in the opposite direction from q to Q. From Eqs. (9), (49) and (64), we can determine the total energy of the reversed dipoles:

$$\Delta E_{Q,q}(r) = 2\,\Delta N_{Q,q}(r) p_D c_0 = \frac{Q\,|q|}{4\pi\varepsilon_0 r}. \tag{65}$$

It is equal to the absolute value of the electrostatic potential energy of a charge q at the electrostatic potential $U_E(r)$ in Eq. (37) of a charge Q.

The evolution of the system is similar to that of the gravitational case in Section 3.1.1; however, attraction and repulsion have to be considered during the approach or separation of bodies C and D. The initial distance between C and D be r, when both bodies are assumed to be at rest, and changes to $r \pm \Delta r$ by the repulsive or attractive force $K_E(r)$ between the charges given by Coulomb's law in Eq. (2) The force is approximately constant for $r \gg \Delta r > 0$ causing accelerations of $b_D = K_E(r)/m_D$ and $b_C = -K_E(r)/m_C$, respectively. Since the duration Δt of the

motions of both bodies is the same, the separation (upper sign) or approach (lower sign) of C and D can be formulated as follows:

$$\pm\Delta r = \pm(s_\mathrm{D} - s_\mathrm{C}) = \pm\frac{1}{2}(b_\mathrm{D} - b_\mathrm{C})(\Delta t)^2 = \frac{1}{2}\left(\frac{1}{m_\mathrm{C}} + \frac{1}{m_\mathrm{D}}\right)K_\mathrm{E}(r)(\Delta t)^2. \tag{66}$$

Comparing the second term of the equation with the last one, it can be seen that $s_\mathrm{D} m_\mathrm{D} = -s_\mathrm{C} m_\mathrm{C}$, i.e. the centre of gravity stays at rest. Multiplication of Eq. (66) by $K_\mathrm{E}(r)$ gives a good estimate of the corresponding kinetic energy:

$$\begin{aligned}\pm\Delta r K_\mathrm{E}(r) = \pm\Delta r\frac{Qq}{4\pi\varepsilon_0 r^2} &= \frac{1}{2}\frac{K_\mathrm{E}^2(r)}{m_\mathrm{B}}(\Delta t)^2 + \frac{1}{2}\frac{K_\mathrm{E}^2(r)}{m_\mathrm{A}}(\Delta t)^2 = \frac{1}{2}m_\mathrm{D}v_\mathrm{D}^2 + \frac{1}{2}m_\mathrm{C}v_\mathrm{C}^2 \\ &= T_\mathrm{D} + T_\mathrm{C} > 0,\end{aligned} \tag{67}$$

where $v_\mathrm{D} = b_\mathrm{D}\Delta t$ and $v_\mathrm{C} = b_\mathrm{C}\Delta t$ are the speeds of the bodies, when the distances $r \pm \Delta r$ between C and D are attained. The sum of the kinetic energies T_C and T_D must, of course, be equal to the difference of the electrostatic potential energy at distances of r and $r \pm \Delta r$:

$$\{U(r) - U(r \pm \Delta r)\}q = \frac{Qq}{4\pi\varepsilon_0}\left(\frac{1}{r} - \frac{1}{r \pm \Delta r}\right) \approx \pm\Delta r\frac{Qq}{4\pi\varepsilon_0 r^2} > 0. \tag{68}$$

The variations of the number of $\Delta N_{Q,q}(r)$ dipoles in Eqs. (58) and (65) during the separation or approach of bodies C and D from r to $r \pm \Delta r$ are

$$\begin{aligned}\delta N_{Q,q}(r, \Delta r) &= \Delta N_{Q,q}(r \pm \Delta r) - \Delta N_{Q,q}(r) \\ &= \frac{\eta_\mathrm{D}\kappa_\mathrm{D}}{c_0^2}\frac{Q|q|}{4\pi}\left[\frac{1}{r \pm \Delta r} - \frac{1}{r}\right] \approx \mp\Delta r\frac{\eta_\mathrm{D}\kappa_\mathrm{D}}{c_0^2}\frac{Q|q|}{4\pi r^2}.\end{aligned} \tag{69}$$

The number of reversed dipoles thus decreases during the separation of C and D in **Figure 5**. The corresponding energy variation with positive q is

$$\delta E_{Q,q}(r, \Delta r) = 2p_\mathrm{D}c_0\,\delta N_{Q,q}(r, \Delta r) = -\Delta r|q|\frac{Q}{4\pi\varepsilon_0 r^2} < 0, \tag{70}$$

cf. Eq. (65). The energy of the reversed dipoles thus decreases by the amount that fuels the kinetic energy in Eq. (67).

In the opposite case with negative q and attraction, it can be seen from **Figure 6** that the increased number of reversed dipoles is actually leaving the system without momentum exchange and is lost. The momentum difference, therefore, is again negative

$$\delta P_{Q,q}(r, \Delta r) = -2p_\mathrm{D}\,\delta N_{Q,q}(r, \Delta r) \tag{71}$$

and so is the energy of the reversed dipoles confined in the system:

$$\delta E_{Q,q}(r, \Delta r) = \delta P_{Q,q}(r, \Delta r)c_0 = -|q|\Delta r\frac{Q}{4\pi\varepsilon_0 r^2} < 0. \tag{72}$$

The electrostatically bound two-body system thus is a closed system in the sense defined by von Laue [49], slowly evolving in time during the movements of bodies C and D. The potential energy converted into kinetic energy stems from the modified dipole distributions.

3.2 Pioneer anomaly

Anomalous frequency shifts of the Doppler radio-tracking signals were detected for both Pioneer spacecraft [56]. The observations of Pioneer 10 (launched on 2 March 1972) published by the Pioneer Team will be considered during the time interval $t_1 - t_0 \approx 11.55\,\text{years} = 3.645 \times 10^8$ s between 3 January 1987 and 22 July 1998, while the spacecraft was at heliocentric distances between $r_0 = 40$ ua and $r_1 = 70.5$ ua. The Pioneer team took into account all known contributions in calculating a model frequency $\nu_{\text{mod}}(t)$ which was based on a constant clock frequency f_0 at the terrestrial control stations. Observations at times $t = t_0 + \Delta t$ then indicated a nearly uniform increase of the observed frequency shift with respect to the expected one of

$$\nu_{\text{obs}}(t) - \nu_{\text{mod}}(t) = 2\dot{f}\,\Delta t \tag{73}$$

with $\dot{f} = 5.99 \times 10^{-9}$ Hz s^{-1} [57].

The observations of the anomalous frequency shifts could, in principle, be interpreted as a deceleration of the heliocentric spacecraft velocity by

$$a_{\text{p}} = -(8.74 \pm 1.33) \times 10^{-10} \text{ m s}^{-2}. \tag{74}$$

However, no unknown sunward-directed force could be identified [58]. Alternatively, a clock acceleration at the ground stations of

$$a_t = \frac{a_{\text{p}}}{c_0} = (2.92 \pm 0.44) \times 10^{-18} \text{ s}^{-1} \tag{75}$$

could explain the anomaly. A true trajectory anomaly together with an unknown systematic spacecraft effect was considered to be the most likely interpretation by Anderson et al. [59]. Although Turyshev et al. [60] later concluded that thermal recoil forces of the spacecraft caused the anomaly of Pioneer 10, the discussion in the literature continued.

Assuming an atomic clock acceleration, a constant reference frequency f_0 for the calculation of $\nu_{\text{mod}}(t)$ is not appropriate. Consequently, we modified in [61] the equation

$$\left[\nu_{\text{obs}}(t) - f_0\right] - \left[\nu_{\text{mod}}(t) - f_0\right] = 2\dot{f}\,\Delta t, \tag{76}$$

equivalent to Eq. (73) with

$$f(t) = f_0 + \dot{f}\,\Delta t = f_0\left(1 + \frac{\dot{f}}{f_0}\,\Delta t\right) = f_0\,(1 + a_t\,\Delta t) \tag{77}$$

and

$$\nu^*_{\text{mod}}(t) = \nu_{\text{mod}}(t) + 2\dot{f}\,\Delta t \tag{78}$$

to

$$\begin{aligned}&\left[\nu_{\text{obs}}(t) - \left(f_0 + \dot{f}\,\Delta t\right)\right] - \left[\nu^*_{\text{mod}}(t) - \left(f_0 + \dot{f}\,\Delta t\right)\right]\\ &\quad = \left[\nu_{\text{obs}}(t) - f(t)\right] - \left[\nu^*_{\text{mod}}(t) - f(t)\right] = 0.\end{aligned} \tag{79}$$

Our gravitationally impact model [16] summarized in Section 2.4 leads to a secular mass increase of massive particles in Eq. (30). Consequently the Rydberg constant in Eq. (32) would increase in a linear approximation with the electron mass m_e according to

$$R_\infty^*(t) = \frac{\alpha^2 c_0}{2h} m_e (1 + A\,\Delta t) \tag{80}$$

resulting in frequency increases of atomic clocks with time. They give rise to the clock acceleration in Eq. (77), if we assume $a_t = A$. The most likely values of $r_{G,e}$ in **Figure 3** range from 2.04×10^{-4} pm to 2.82 fm, the classical electron radius, corresponding with Eq. (31) to $A_H = 2.43 \times 10^{-18}\ \mathrm{s}^{-1} \approx H_0$, the Hubble constant, and $A \approx 1.3 \times 10^{-20}\ \mathrm{s}^{-1}$. Within the uncertainty margins, the high value agrees with a_t in Eq. (75) and would quantitatively account for the Pioneer frequency shift. Should the anomaly be much less pronounced, because thermal recoil forces decelerate the spacecraft, the range of $r_{G,e}$ in **Figure 3** could accommodate smaller values of a_t as well.

3.3 Sun-Earth distance increase

A secular increase of the mean Sun-Earth distance with a rate of (15 ± 4) m per century had been reported using many planetary observations between 1971 and 2003 [45]. Neither the influence of cosmic expansion nor a time-dependent gravitational constant seems to provide an explanation [62].

As our impact model summarized in Section 2.4 leads to a secular mass increase according to Eq. (30) of all massive bodies fuelled by a decrease in energy of the background flux of gravitons, it allowed us to formulate a quantitative understanding of the effect within the parameter range of the model [63].

The value of the astronomical unit is defined by the International Astronomical Union (IAU) and the Bureau International des Poids et Mesure [64] as $1\ \mathrm{ua} = 1.495\,978\,707 \times 10^{11}$ m (exact). The mean Sun-Earth distance r_E is known with a standard uncertainty of (3 to 6) m [65–67].

Considering this uncertainty, the measurement of a change rate of

$$\frac{\Delta r_E}{\Delta t} = \frac{(15 \pm 4)\ \mathrm{m}}{3.156 \times 10^9\ \mathrm{s}} = (4.8 \pm 1.3)\ \mathrm{nm\ s^{-1}} \tag{81}$$

is difficult but feasible as relative determination. A circular orbit approximation had been considered, because the mean value of r_E is of interest:

$$r_E = \frac{G_N M_\odot}{v_E^2} = \frac{\mu_\odot}{v_E^2}. \tag{82}$$

This follows from equating the gravitational attraction, cf. Eq. (1), and the centrifugal force with v_E, the tangential orbital velocity of the Earth, where the heliocentric gravitational constant is $\mu_\odot = 1.327\,124\,400\,42 \times 10^{20}\ \mathrm{m^3\ s^{-2}}$ (IAU) and the mass of the Sun $M_\odot = 1.988\,42 \times 10^{30}$ kg.

We now consider Eq. (82) not only for t_0 but also at $t = t_0 + \Delta t$ assuming constant G_N as well as constant v_E. The latter assumption is justified by the fact that any uniformly moving particle does not experience a deceleration. It implies an increase of the momentum together with the mass accumulation of the Earth. The apparent violation of the momentum conversation principle can be resolved by considering the accompanying momentum changes of the graviton distribution. A detailed discussion of this aspect is given in Section 3 of [16].

From Eqs. (30) and (82), it follows

$$r_{\mathrm{E}}(t) = r_{\mathrm{E}} + \Delta r_{\mathrm{E}} \approx \frac{G_{\mathrm{N}}}{v_{\mathrm{E}}^2} M_{\odot} (1 + A\,\Delta t) \tag{83}$$

and

$$\frac{\Delta r_{\mathrm{E}}}{\Delta t} \approx r_{\mathrm{E}} A. \tag{84}$$

With the help of Eqs. (31) and (81), the electron mass radius can now be calculated. The result is

$$r_{\mathrm{G},e} = \left(r_{\mathrm{E}} \frac{\Delta t}{\Delta r_{\mathrm{E}}}\ 1.014 \times 10^{-49}\ \mathrm{m}^2\ \mathrm{s}^{-1} \right)^{-1/2} = \left(1.8^{+0.4}_{-0.2}\right)\ \mathrm{fm}, \tag{85}$$

close to the classical electron radius

$$r_{\mathrm{e}} = \alpha^2 a_0 = 2.82\ \mathrm{fm}. \tag{86}$$

The relative accumulation rate deduced from the observations of r_{E} finally becomes $A = A_{ua} \approx 3.2 \times 10^{-20}\ \mathrm{s}^{-1}$ (see **Figure 3**).

3.4 Secular perihelion advances in the solar system

Multiple applications of the interaction process described in Section 2.4 can produce gravitons with reduction parameters greater than Y in large mass conglomerations—within the Sun in this section. The proportionality of the linear term in the binomial theorem with the exponent n in

$$(1 - Y)^n \approx 1 - nY \quad \text{for } Y \ll 1 \tag{87}$$

suggests that a linear superposition of the effects of multiple interactions will be a good approximation, if n is not too large. Energy reductions according to Eq. (18) are therefore not lost, as claimed by Drude [21], but they are redistributed to other emission locations within the Sun. This has two consequences: (1) the total energy reduction is still dependent on the solar mass, and (2) since emissions from matter closer to the surface of the Sun in the direction of an orbiting object is more likely to escape into space than gravitons from other locations, the effective gravitational centre should be displaced from the centre of the Sun towards that object.

Using published data on the secular perihelion advances of the inner planets Mercury, Venus, Earth and Mars of the solar system and the asteroid Icarus, we found that the effective gravitational centre is displaced from the centre of the Sun by approximately $\rho = 4400$ m [68]. Since an analytical derivation of this value from the mass distribution of the Sun was beyond the scope of the study, future investigations need to show that the modified process with directed secondary graviton emission can quantitatively account for such a displacement.

3.5 Planetary flyby anomalies

3.5.1 Earth flybys

Several Earth flyby manoeuvres indicated anomalous accelerations and decelerations and led to many investigations without reaching a solution of the problem

(see recent reviews by Anderson et al. [69] and Nieto and Anderson [70]). Since there is general agreement that the anomaly is only significant near perigee, we discuss here the seven passages at altitudes below 2000 km listed in Table 1 of Acedo [71]. Three of them (Galileo I, NEAR and Rosetta) we have studied in [72] assuming the gravitational impact model of Section 2.4 and multiple interactions. As in Section 3.4, the multiple interactions result in a deviation ρ of the effective gravitational centre from the geometric centre. We obtained for Galileo, NEAR and Rosetta $\rho \approx 1.3$ m, 3.9 m and 0.5 m, respectively. The study had been conducted assuming a spherically symmetric emission of liberated gravitons mentioned in Section 2.4.

With the assumption of an *antiparallel* emission, we have repeated the analysis and found $\rho \approx 2$ m for all spacecraft, provided the origin of ρ is shifted by approximately -0.6 m in the direction of the perigee of Galileo I, $+1.9$ m for NEAR and -1.5 m for Rosetta. Moreover, it was possible to model the decelerations of Galileo II on 8 December 1992 with a shift of -3.4 m, of Cassini on 18 August 1999 with -2.7 m and the null result for Juno on 9 October 2013 with -2 m.

An origin offset of $+3.4$ m opposite to the Cassini perigee could to a first approximation achieve all apparent shifts taking the geographic coordinates of the various flybys into account. A detailed study would have to consider in addition the Earth gravitational model.

3.5.2 Juno Jupiter flybys

Juno was inserted into an elliptical orbit around Jupiter on 4 July 2016 with an orbital period of 53.5 days. Acedo et al. [74] studied the first and the third orbit with a periapsis of "4200 km over the planet top clouds". "A significant radial component was found and this decays with the distance to the center of Jupiter as expected from an unknown physical interaction ... . The anomaly shows an asymmetry among the incoming and outgoing branches of the trajectory ... ". The radial component is shown in their **Figure 6** in the time interval $t = (-180 \text{ to } +180)$ min around perijove for the first and third Juno flyby. The peak anomalous outward accelerations shown are in both cases: $\delta a = 7$ mm s^{-2} at $t \approx -15$ min and $\delta a = 6$ mm s^{-2} at $t \approx +17$ min.

We applied the multiple-interaction concept of the previous Sections 3.4 and 3.5.1 in [75] and found that offsets of $\rho \approx$ (8 to 27) km of the gravitational from the geometric centre are required to model the acceleration in **Figure 7**, which is in good agreement with the observations during the Juno Jupiter flybys. The variation of ρ could be modelled by an ellipsoidal displacement of the gravitational centre offset in the direction of a flyby position near $t = -10$ min.

3.6 Rotation velocities of spiral galaxies

The rotation velocities of spiral galaxies are difficult to reconcile with the Keplerian motions, if only the gravitational effects of the visible matter are taken into account, cf. [76, 77]. Dark matter had been proposed by Oort [78] and Zwicky [79] in order to understand several velocity anomalies in galaxies and clusters of galaxies. A Modification of the Newtonian Dynamics (MOND) has been introduced by Milgrom [80] that assumes a modified gravitational interaction at low acceleration levels.

The impact model of gravitation in Section 2.4 is applied to the radial acceleration of disk galaxies [81]. The flat velocity curves of NGC 7814, NGC 6503 and M 33 are obtained without the need to postulate any dark matter contribution. The concept explained below provides a physical process that relates the fit parameter of

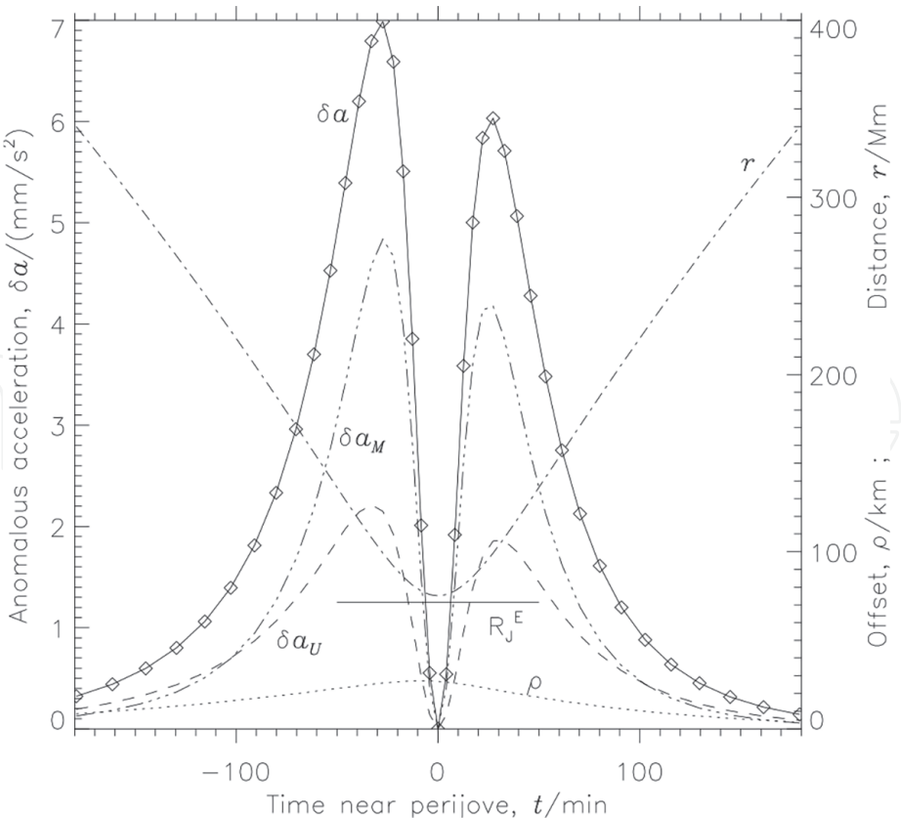

Figure 7.
*Anomalous radial outward acceleration δa experienced by Juno near the perijove at time t = 0 (solid curve with diamond signs). It is composed of δa_U calculated from the adjusted potential and δa_M calculated from the adjusted centrifugal energy (see effective potential energy equation 14 of [73]). A multi-interaction process has been assumed within the mass 1.89858×10^{27} kg of Jupiter. It causes an offset ρ of the effective pivotal point of the gravitational attraction from the geometric centre of Jupiter (dotted curve). Also shown are the equatorial radius of Jupiter R_J^E (solid bar) and the radial distance r of Juno from the centre (dash-dot curve) (***Figure 7*** of [75]).*

the acceleration scale defined by McGaugh et al. [82] to the mean-free path length of gravitons in the disks of galaxies. It may also provide an explanation for MOND.

McGaugh [83] has observed a fine balance between baryonic and dark mass in spiral galaxies that may point to new physics for DM or a modification of gravity. Fraternali et al. [84] have also concluded that either the baryons dominate the DM or the DM is closely coupled with the luminous component. Salucci and Turini [85] have suggested that there is a profound interconnection between the dark and the stellar components in galaxies.

The large baryonic masses in galaxies will cause multiple interactions of gravitons with matter if their propagation direction is within the disk. For each interaction the energy loss of the gravitons is assumed to be YT_G (for details see Section 2.3 of [16]). The important point is that the multiple interactions occur only in the galactic plane and not for inclined directions. An interaction model is designed indicating that an amplification factor of approximately two can be achieved by six successive interactions. An amplification occurs for four or more interactions. The process works, of course, along each diameter of the disk and leads to a two-dimensional distribution of reduced gravitons.

The multiple interactions do not increase the total reduction of graviton energy, because the number of interactions is determined by the (baryonic) mass of the gravitational centre according to [16]. A galaxy with enhanced gravitational acceleration in two dimensions defined by the galactic plane will, therefore, have a reduced acceleration in directions inclined to this plane.

3.7 Light deflection and Shapiro delay

The deflection of light near gravitational centres is of fundamental importance. For a beam passing close to the Sun, Soldner [86] and Einstein [87] obtained a deflection angle of $0.87''$ under the assumption that radiation would be affected in the same way as matter. *Twice* this value was then derived in the framework of the GTR [2][4] and later by Schiff [88] using the equivalence principle and STR. The high value was confirmed during the total solar eclipse in 1919 for the first time [89]. This and later observations have been summarized by Mikhailov [90] and combined to a mean value of approximately $2''$.

The deflection of light has also been considered in the context of the gravitational impact model summarized in Section 2.4. As a secular mass increase of matter was a consequence of this model, the question arises on how the interaction of gravitons with photons can be understood, since the photon mass is in all likelihood zero.[5] An initial attempt at solving that problem has been made in [91], where we assumed that a photon stimulates an interaction with a rate equal to its frequency $\nu = E_\nu/h$. It is summarized here under the assumption of an *antiparallel* re-emission, both for massive particles and photons.

A physical process will then be outlined that provides information on the gravitational potential U at the site of a photon emission [95]. This aspect had not been covered in our earlier paper on the gravitational redshift [96].

Interactions between massive bodies have been treated in [16] with an absorption rate of *half* the intrinsic de Broglie frequency of a mass, because *two* virtual gravitons have to be emitted for one interaction. The momentum transfer to a photon will thus be twice as high as to a massive body with a mass equivalent to E_ν/c_0^2.

We then apply the momentum conservation principle to photon-graviton pairs in the same way as to photons [73] and can write after a reflection of $\boldsymbol{p}_\mathrm{G}$

$$\boldsymbol{p}_\nu + \boldsymbol{p}_\mathrm{G} = \boldsymbol{p}_\nu + 2\,\boldsymbol{p}_\mathrm{G} - \boldsymbol{p}_\mathrm{G} = \boldsymbol{p}_\nu^{\,*} - \boldsymbol{p}_\mathrm{G} \tag{88}$$

with $|\boldsymbol{p}_\mathrm{G}| = p_\mathrm{G} = T_\mathrm{G}/c_0$.

We assume, applying Eq. (88) with $p_\mathrm{G} \ll p_\nu = |\boldsymbol{p}_\nu|$, that under the influence of a gravitational centre relevant interactions occur on opposite sides of a photon with p_G and $p_\mathrm{G}(1-Y)$ transferring a net momentum of $2Yp_\mathrm{G}$. Note, in this context, that the Doppler effect can only operate for interactions of photons with massive bodies [97, 98]. Consequently, there will be no energy change of the photon, because both gravitons are reflected with constant energies under these conditions, and we can write for a pair of interactions:

$$E_\nu = |\boldsymbol{p}_\nu|c = |\boldsymbol{p}_\nu + 2Y\boldsymbol{p}_\mathrm{G}|c' = |\boldsymbol{p}_\nu|c' = E'_\nu, \tag{89}$$

where $\boldsymbol{p}'_\nu$ is the photon momentum after the events. If $\boldsymbol{p}_\nu$ and a component of $2Y\boldsymbol{p}_\mathrm{G}$ are pointing in the same direction, it is $c' < c$, the speed is reduced; an antiparallel direction leads to $c' > c$. Note that this could, however, not result in

[4] It is of interest in the context of this paper that Einstein employed Huygens' principle in his calculation of the deflection.

[5] A zero mass of photons follows from the STR and a speed of light in vacuum c_0 constant for all frequencies. Einstein [52] used "Lichtquant" for a quantum of electromagnetic radiation; the term "photon" was introduced by Lewis [15]. With various methods the photon mass could be constrained to $m_\nu < 10^{-49}$ kg [92, 93] or even to $m_\nu < 6.3 \times 10^{-53}$ kg [94].

$c' > c_0$, because $c = c_0$ can only be attained in a region with an isotropic distribution of gravitons with a momentum of p_G, i.e. with a gravitational potential $U_0 = 0$.

The momentum $\boldsymbol{p}_\nu$ of a photon radially approaching a gravitational centre will be treated in line with Eq. (6) of [17] for massive bodies, however, with twice the rate of interaction. Since we know from observations that the deflection of light near the Sun is very small, the momentum variation caused by the weak and static gravitational interaction is also very small. The momentum change rate of the photon can then be approximated by

$$\frac{\delta \boldsymbol{p}_\nu}{\Delta t} \approx 2 G_N M_\odot \frac{\hat{\boldsymbol{r}}}{r^2} \frac{p_\nu}{c_0}, \tag{90}$$

where $r = |\boldsymbol{r}|$ is the distance of the photon from the centre, and the position vector of the photon is $r\hat{\boldsymbol{r}}$ with a unit vector $\hat{\boldsymbol{r}}$. The small deflection angle also allows an approximation of the actual path by a straight line along an x axis: $x \approx c_0 t$. The normalized momentum variation along the trajectory then is

$$\frac{\delta p_\nu}{p_\nu} \cos\vartheta \approx \frac{2 G_N M_\odot}{c_0} \frac{x}{r^3} \Delta t. \tag{91}$$

The corresponding component perpendicular to the trajectory is

$$\frac{\delta p_\nu}{p_\nu} \sin\vartheta \approx \frac{2 G_N M_\odot}{c_0} \frac{R}{r^3} \Delta t, \tag{92}$$

where R is the impact parameter of the trajectory. Integration of Eq. (91) over t from $-\infty$ to x/c_0 (for details see [17]) yields

$$\frac{\left[\Delta \boldsymbol{p}_\nu(r)\right]_x}{p_\nu} \approx \frac{2 G_N M_\odot}{c_0^2 r} = \frac{2 G_N M_\odot}{c_0^2 \sqrt{R^2 + x^2}}. \tag{93}$$

If we apply Eq. (89) to a photon approaching the Sun along the x axis starting from infinity with $E_\nu = p_\nu c_0$, and considering that the y component in Eq. (91) is much smaller than the x component in Eq. (92) for $x \gg R$, the photon speed $c(r)$ as a function of r can be determined from

$$p_\nu c_0 \approx \left\{ p_\nu + \left[\Delta \boldsymbol{p}_\nu(r)\right]_x \right\} c(r). \tag{94}$$

Division by p_ν then gives with Eq. (93)

$$\frac{1}{[n_G(r)]_x} = \frac{c(r)}{c_0} \approx 1 - \frac{2 G_N M_\odot}{c_0^2 r} = 1 + \frac{2U(r)}{c_0^2} \tag{95}$$

as a good approximation of the inverse gravitational index of refraction along the x axis. The same index has been obtained albeit with different arguments, e.g. in [99, 100]. The resulting speed of light is in agreement with evaluations by Schiff [88], for a radial propagation[6] in a central gravitational field, and Okun [101] —calculated on the basis of the standard Schwarzschild metric. A decrease of the speed of light near the Sun, consistent with Eq. (95), is not only supported by the

[6] Einstein [108] states explicitly that the speed at a certain location is not dependent on the direction of the propagation.

predicted and subsequently observed Shapiro delay [102–107] but also indirectly by the deflection of light [89].

The deflection of light by gravitational centres according to the GTR [2] and its observational detection by Dyson et al. [89] leave no doubt that a photon is deflected by a factor of two more than the expected relative to a corresponding massive particle. Since in our concept the interaction rate between photons and gravitons is twice as high as for massive particles of the same total energy, the reflection of a graviton from a photon with a momentum of $(1 - Y)p_G$ must also be *antiparallel* to the incoming one, i.e. a momentum of $-2Yp_G$ will be transferred. Otherwise the correct deflection angle for photons cannot be obtained. This modified interaction process has one further important advantage: the reflected graviton can interact with the deflecting gravitational centre and transfers $2Yp_G$—through the process outlined in the paragraph just before Eq. (48)—in compliance with the momentum conservation principle. In the old scheme, the violation of this principle had no observational consequences, because of the extremely large masses of relevant gravitational centres, but the adherence to both the momentum and energy conservation principles is very encouraging and clearly favours the new concept.

Basically the same arguments are relevant for the longitudinal interaction between photons and gravitons. The momentum transfer per interaction will be doubled, but the gravitational absorption coefficient will be reduced by a factor of two. Together with an increased graviton density, all quantities and results are the same as before. However, a detailed analysis shows that the momentum conservation principle is now also adhered to.

3.8 Gravitational redshift

The gravitational potential U at a distance r from a spherical body with mass M is constraint in the weak-field approximation for nonrelativistic cases by

$$-1 \ll \frac{U}{c_0^2} = -\frac{G_N M}{c_0^2\, r} \leq 0 \tag{96}$$

cf. [73]. A definition of a reference potential in line with this formulation is $U_\infty = 0$ for $r = \infty$.

The study of the gravitational redshift, predicted for solar radiation by Einstein [109], is still an important subject in modern physics and astrophysics [95, 96, 110–114]. This can be exemplified by two conflicting statements. Wolf et al. [10] write: "The clock frequency is sensitive to the gravitational potential U and not to the local gravity field $\boldsymbol{g} = \nabla U$". Whereas it is claimed by Müller et al. [11]: "We first note that no experiment is sensitive to the absolute potential U".

Support for the first alternative can be found in many publications [49, 88, 95, 96, 109, 115–117], but it is, indeed, not obvious how an atom can locally sense the gravitational potential U. Experiments on Earth, in space and in the Sun-Earth system, cf. [118–123], however, have quantitatively confirmed in the static weak field approximation a relative frequency shift of

$$\frac{\nu - \nu_0}{\nu_0} = \frac{\Delta\nu}{\nu_0} \approx \frac{\Delta U}{c_0^2} = \frac{U - U_0}{c_0^2}, \tag{97}$$

where ν_0 is the frequency of the radiation emitted by a certain transition at U_0 and ν is the observed frequency there, if the emission caused by the same transition had occurred at a potential U.

Since Einstein discussed the gravitational redshift and published conflicting statements regarding this effect in [2, 87, 109], the confusion could still not be cleared up consistently, cf., e.g. [124, 125]. In most of his publications Einstein defined clocks as atomic clocks. Initially he assumed that the oscillation of an atom corresponding to a spectral line might be an intra-atomic process, the frequency of which would be determined by the atom alone. Scott [126] also felt that the equivalence principle and the notion of an ideal clock running independently of acceleration suggest that such clocks are unaffected by gravity. Einstein [2] later concluded that clocks would slow down near gravitational centres, thus causing a redshift.

The question whether the gravitational redshift is caused by the emission process (case a) or during the transmission phase (case b) is nevertheless still a matter of recent debates. Proponents are, e.g. of (a) Schiff [88], Okun et al. [116], Møller [127], Cranshaw et al. [128] and Ohanian [129], and of (b) Hay et al. [130], Straumann [131], Randall [132] and Will [133]. It is surprising that the same team of experimenters albeit with different first authors published different views in [128, 130] on the process of the Pound-Rebka-Experiment.

Pound and Snider [120] and Pound [134] pointed out that this experiment could not distinguish between the two options, because the invariance of the velocity of the radiation had not been demonstrated.

Einstein [13] emphasized that for an elementary emission process, not only the energy exchange but also the momentum transfer is of importance; see also [12, 46, 97]. Taking these considerations into account, we formulated a photon emission process at a gravitational potential U assuming that:

1. The atom cannot sense the potential U, in line with the original proposal by Einstein [87, 109], and initially emits the same energy ΔE_0 at $U < 0$ and $U_0 = 0$.

2. It also cannot directly sense the speed of light at the location with a potential U. The initial momentum thus is $p_0 = \Delta E_0/c_0$.

3. As the local speed of light is, however, $c(U) \neq c_0$, a photon having an energy of ΔE_0 and a momentum p_0 is not able to propagate. The necessary adjustments of the photon energy and momentum as well as the corresponding atomic quantities then lead in the interaction region to a redshift consistent with $h\nu = \Delta E_0 \left(1 + U/c_0^2\right)$ and observations [96].

As outlined in Section 3.7, there is general agreement in the literature that the local speed of light is

$$c(U) \approx c_0 \left(1 + \frac{2U}{c_0^2}\right) \tag{98}$$

in line with Eq. (95) in Section 3.7. It has, however, to be noted that the speed $c(U)$ was obtained for a photon propagating from U_0 to U, and, therefore, the physical process which controls the speed of newly emitted photons at a gravitational potential U is not yet established.

An attempt to do that will be made by assuming an aether model. Before we suggest a specific aether model, a few statements on the aether concept in general should be mentioned. Following Michelson and Morley [135] famous experiment, Einstein [51, 109] concluded that the concept of a light aether as carrier of the electric and magnetic forces is not consistent with the STR. In response to critical remarks by Wiechert [136], cf. Schröder [137] for Wiechert's support of the aether,

von Laue [138] wrote that the existence of an aether is not a physical, but a philosophical problem, but later differentiated between the physical world and its mathematical formulation [139]: a four-dimensional "world" is only a valuable mathematical trick; a deeper insight, which some people want to see behind it, is not involved.

In contrast to his earlier statements, Einstein said at the end of a speech in Leiden that according to the GTR, a space without aether cannot be conceived [140] and even more detailed thus one could instead of talking about "aether" as well discuss the "physical properties of space". In theoretical physics we cannot do without aether, i.e. a continuum endowed with physical properties [141]. Michelson et al. [142] confessed at a meeting in Pasadena in the presence of H.A. Lorentz that he clings a little to the aether, and Dirac [143] wrote in a letter to *Nature* that there are good reasons for postulating an aether.

In [17] we proposed an impact model for the electrostatic force based on massless dipoles. The vacuum is thought to be permeated by these dipoles that are, in the absence of electromagnetic or gravitational disturbances, oriented and directed randomly propagating along their dipole axis with a speed of c_0. There is little or no interaction among them. We suggest to identify the dipole distribution postulated in Section 2.5 with an aether. Einstein's aether mentioned above may, however, be more related to the gravitational interactions, cf. [144]. In this case, we have to consider the graviton distribution as another component of the aether.

We now assume that an individual dipole interacts with gravitons in the same way as photons in Eq. (89), i.e. according to

$$T_{\mathrm{D}} = |\boldsymbol{p}_{\mathbf{D}}|c = |\boldsymbol{p}_{\mathbf{D}} + 2Y\boldsymbol{p}_{\mathbf{G}}|c' = |\boldsymbol{p}'_{\mathbf{D}}|c' = T'_{\mathrm{D}}, \tag{99}$$

where T_{D} and $\boldsymbol{p}_{\mathbf{D}}$ refer to the energy and momentum of a dipole. The condition $p_{\mathrm{D}} \gg p_{\mathrm{G}}$, cf. Eq. (88), is fulfilled in the range from $Y \approx 10^{-22}$ to 10^{-15} for all $r_{\mathrm{e}} \leq 2.82$ fm (see Section 2.5 and **Figure 3**).

We can then modify Eqs. (90)–(94) by changing ν to D and find that Eqs. (95) and (98) are also valid for dipoles with a speed of c_0 for $U_0 = 0$.

Considering that many suggestions have been made to describe photons as solitons, e.g. in [145–150], we also propose that a photon is a soliton propagating in the dipole aether with a speed of $c(U)$, cf. Eq. (98), controlled by the dipoles moving in the direction of propagation of the photon. The dipole distribution thus determines the gravitational index of refraction, cf. Eq. (95), and consequently the speed of light $c(U)$ at the potential U. This solves the problem formulated in relation to Eq. (98) and might be relevant for other phenomena, such as gravitational lensing and the cosmological redshift, cf., e.g. [151]. Should the speculation in Section 2.5.2 be taken seriously that the dipole distribution corresponds to DM, it has to be much more evenly distributed than previously thought [152]. The light deflection would then be caused by gravitationally induced index of refraction variations.

4. Discussion and conclusions

With Newton's law of gravitation as starting point, the ideas presented in Section 2.4 allow an understanding of far-reaching gravitational force between massive particles as local interactions of hypothetical massless gravitons travelling with the speed of light in vacuum. The gravitational attraction leads to a general mass accretion of massive particles with time, fuelled by a decrease of the graviton energy density in space. The physical processes during the conversion of gravitational potential energy into kinetic energy have been described for two bodies with

masses m_A and m_b, and the source of the potential energy could be identified in Section 3.1.1. In order to avoid conflicts with energy and momentum conservation, we had to modify a detail of the interaction process in Eq. (26), i.e. assume an *antiparallel* emission of the secondary graviton with respect to the incoming one.

Multiple interactions of gravitons leading to shifts of the effective gravitational centre of a massive body from the "centre of gravity" are treated in Sections 3.4–3.6 taking the modified concept into account. The interaction of gravitons with photons in Section 3.7 had to be modified as well, but the modification did not change the results, with the exception that now, both the energy and momentum conservation principles are fulfilled.

Our main aim in Section 3.8 was to identify a physical process that leads to a speed $c(U)$ of photons controlled by the gravitational potential U. This could be achieved by postulating an aether model with moving dipoles, in which a gravitational index of refraction $n_G(U) = c_0/c(U)$ regulates the emission and propagation of photons as required by energy and momentum conservation principles. The emission process thus follows Steps (1) to (3) in Section 3.8, where the local speed of light is given by the gravitational index of refraction n. In this sense, the statement that an atom cannot detect the potential U by Müller et al. [11] is correct; the local gravity field $\boldsymbol{g}$, however, is not controlling the emission process.

A photon will be emitted by an atom with appropriate energy and momentum values, because the local speed of light requires an adjustment of the momentum. This occurs in the interaction region between the atom and its environment as outlined in Step 3.

In the framework of a recently proposed electrostatic impact model in [17], the physical processes related to the variation of the electrostatic potential energy of two charged bodies have been described, and the "source region" of the potential energy in such a system could be identified and is summarized in Section 3.1.2.

Sotiriou et al. [125] made a statement in the context of gravitational theories in "A no-progress report": "[...] it is not only the mathematical formalism associated with a theory that is important, but the theory must also include a set of rules to interpret physically the mathematical laws". With this goal in mind, we have presented our ideas on the gravitational and electrostatic interactions.

Acknowledgements

This research has made extensive use of the Smithsonian Astrophysical Observatory (SAO)/National Aeronautics and Space Administration Astrophysics Data System (NASA/ADS). Administrative support has been provided by the Max-Planck-Institute for Solar System Research and the Indian Institute of Technology (Banaras Hindu University).

Author details

Klaus Wilhelm[1†] and Bhola N. Dwivedi[2*†]

1 Max-Planck-Institut für Sonnensystemforschung (MPS), Göttingen, Germany

2 Department of Physics, Indian Institute of Technology (Banaras Hindu University), Varanasi, India

*Address all correspondence to: bnd.app@iitbhu.ac.in

† These authors contributed equally.

References

[1] Mohr PJ, Newell DB, Taylor BN. CODATA recommended values of the fundamental physical constants: 2014. Reviews of Modern Physics. 2016;**88**: 035009

[2] Einstein A. Die Grundlage der allgemeinen Relativitätstheorie. Annalen der Physik (Leipzig). 1916;**354**: 769-822

[3] Planck M. Zur Theorie der Wärmestrahlung. Annalen der Physik (Leipzig). 1909;**336**:758-768

[4] Wheeler JA, Feynman RP. Classical electrodynamics in terms of direct interparticle action. Reviews of Modern Physics. 1949;**21**(3):425-433

[5] Schwarzschild K. Zur Elektrodynamik. II. Die elementare elektrodynamische Kraft. Nachrichten von der Gesellschaft der Wissenschaften zu Göttingen, Mathematisch-Physikalische Klasse. 1903;**3**:132-141

[6] Lange M. The most famous equation. Journal of Philosophy. 2001;**98**:219-238

[7] von Laue M. Das Relativitätsprinzip. Braunschweig: Friedr. Vieweg & Sohn; 1911

[8] Penrose R. The Road to Reality: A Complete Guide to the Laws of the Universe. New York: Alfred A. Knopf; 2006

[9] Carlip S. Kinetic energy and the equivalence principle. American Journal of Physics. 1998;**66**:409-413

[10] Wolf P, Blanchet L, Bordé CJ, Reynaud S, Salomon C, Cohen-Tannoudji C. Atom gravimeters and gravitational redshift. Nature. 2010;**467**:E1

[11] Müller H, Peters A, Chu S. Müller, Peters & Chu reply. Nature. 2010; **467**:E2

[12] Poincaré H. La théorie de Lorentz et le principe de réaction. Archives Néerlandaises des Sciences Exactes et Naturelles. 1900;**5**:252-278

[13] Einstein A. Zur Quantentheorie der Strahlung. Physikalische Zeitschrift. 1917;**XVIII**:121-128

[14] Compton AH. A quantum theory of the scattering of X-rays by light elements. Physical Review. 1923;**21**: 483-502

[15] Lewis GN. The conservation of photons. Nature. 1926;**118**:874-875

[16] Wilhelm K, Wilhelm H, Dwivedi BN. An impact model of Newton's law of gravitation. Astrophysics and Space Science. 2013; **343**:135-144

[17] Wilhelm K, Dwivedi BN, Wilhelm H. An impact model of the electrostatic force: Coulomb's law re-visited. arXiv1403.1489v5. 2014 [Accessed: 26 October 2019]

[18] Fatio de Duilleir N. De la cause de la pesanteur. (Ed. Karl Bopp). Notes and Records of the Royal Society of London. 1949;**6**:125-160

[19] Bopp K. Fatio de Duillier: De la cause de la pesanteur. Schriften der Straßburger Wissenschaftlichen Gesellschaft Heidelberg. 1929;**10**:19-66

[20] Zehe H. Die Gravitationstheorie des Nicolas Fatio de Duillier. Archive for History of Exact Sciences. 1983;**28**:1-23

[21] Drude P. Ueber Fernewirkungen. Annalen der Physik (Leipzig). 1897; **268**(12):I-XLIX

[22] Weinberg S. Photons and gravitons in S-matrix theory: Derivation of charge conservation and equality of

gravitational and inertial mass. Physical Review. 1964;**135**:B1049-B1056

[23] Jackson JD. Classical Electrodynamics. 3rd ed. New York, Chichester, Weinheim, Brisbane, Singapore, Toronto: John Wiley & Sons, Inc; 1999

[24] Jackson JD. Klassische Elektrodynamik. 4. Auflage ed. Berlin, New York: Walter de Gruyter; 2006

[25] Newell DB, Cabiati F, Fischer J, Fujii K, Karshenboim SG, Margolis HS, et al. The CODATA 2017 values of h, e, k, and N_A for the revision of the SI. Metrologia. 2018;**55**:L13-L16

[26] Weizsäcker CFV. Ausstrahlung bei Stößen sehr schneller Elektronen. Zeitschrift für Physik. 1934;**88**:612-625

[27] Yukawa H. On the interaction of elementary particles I. Proceedings of the Physico-Mathematical Society of Japan 3rd Series. 1935;**17**:48-57

[28] Nimtz G, Stahlhofen AA. Universal tunneling time for all fields. Annalen der Physik (Berlin). 2008;**17**:374-379

[29] Mandelstam LI, Tamm IE. The uncertainty relation between energy and time in non-relativistic quantum mechanics. Journal of Physics (USSR). 1945;**9**:249-254

[30] Aharonov Y, Bohm D. Time in the quantum theory and the uncertainty relation for time and energy. Physical Review. 1961;**122**:1649-1658

[31] Hilgevoord J. The uncertainty principle for energy and time. II. American Journal of Physics. 1998; **66**(5):396-402

[32] Bohr N. Discussions with Einstein on epistemological problems in atomic physics. In: Albert Einstein: Philosopher-Scientist. Cambridge: Cambridge University Press; 1949

[33] Low FE, Mende PF. A note on the tunneling time problem. Annals of Physics (N.Y.). 1991;**210**:380-387

[34] Stahlhofen AA, Nimtz G. Evanescent modes are virtual photons. Europhysics Letters. 2006;**76**:189-195

[35] de Broglie L. Ondes et quanta. Comptes Rendus. 1923;**177**:507-510

[36] Schrödinger E. Über die kräftefreie Bewegung in der relativistischen Quantenmechanik. Sitzungsberichte der Preussischen Akademie der Wissenschaften. Physikalisch-Mathematische Klasse. 1930:418-431

[37] Schrödinger E. Zur Quantendynamik des Elektrons, Sitzungsberichte der Preussischen Akademie der Wissenschaften. Physikalisch-Mathematische Klasse. 1931:63-72

[38] Huang K. On the zitterbewegung of the Dirac electron. American Journal of Physics. 1952;**20**:479-484

[39] Hestenes D. The Zitterbewegung interpretation of quantum mechanics. Foundations of Physics. 1990;**20**: 1213-1232

[40] Einstein A. Ist die Trägheit eines Körpers von seinem Energieinhalt abhängig? Annalen der Physik (Leipzig). 1905;**323**:639-641

[41] Fahr H-J, Heyl M. Cosmic vacuum energy decay and creation of cosmic matter. Naturwissenschaften. 2007;**94**: 709-724

[42] Fahr H-J, Siewert M. Local spacetime dynamics, the Einstein-Straus vacuole and the Pioneer anomaly: A new access to these problems. Zeitschrift für Naturforschung. 2007;**62a**:117-126

[43] Fahr H-J. Universum ohne Urknall. Kosmologie in der Kontroverse.

Spektrum Akademischer Verlag: Berlin, Heidelberg, Oxford; 1995

[44] Beck C, Mackey MC. Could dark energy be measured in the lab? Physics Letters B. 2005;**605**:295-300

[45] Krasinsky GA, Brumberg VA. Secular increase of astronomical unit from analysis of the major planet motions, and its interpretation. Celestial Mechanics and Dynamical Astronomy. 2004;**90**:267-288

[46] Abraham M. Prinzipien der Dynamik des Elektrons. Annalen der Physik (Leipzig). 1902;**315**:105-179

[47] Wilhelm K, Dwivedi BN. On the potential energy in a gravitationally bound two-body system. New Astronomy. 2015;**34**:250-252

[48] Brillouin L. The actual mass of potential energy, a correction to classical relativity. Proceedings of the National Academy of Sciences. 1965;**53**:475-482

[49] von Laue M. Zur Theorie der Rotverschiebung der Spektrallinien an der Sonne. Zeitschrift für Physik. 1920; **3**(5):389-395

[50] Wilhelm K, Dwivedi BN. On the potential energy in a gravitationally bound two-body system with arbitrary mass distribution. arXiv:1502.05662v2. 2015 [Accessed: 26 October 2019]

[51] Einstein A. Zur Elektrodynamik bewegter Körper. Annalen der Physik (Leipzig). 1905;**322**:891-921

[52] Einstein A. Über einen die Erzeugung und Verwandlung des Lichtes betreffenden heuristischen Gesichtspunkt. Annalen der Physik (Leipzig). 1905;**322**:132-148

[53] Okun LB. Mass versus relativistic and rest masses. American Journal of Physics. 2009;**77**:430-431

[54] Hund F. Theoretische Physik. Band 2, 3. Auflage. Stuttgart: B.G. Teubner Verlagsgesellschaft; 1957

[55] Wilhelm K, Dwivedi BN. On the potential energy in an electrostatically bound two-body system. arXiv: 1501.05615. 2014 [Accessed: 30 October 2019]

[56] Anderson JD, Laing PA, Lau EL, Liu AS, Nieto MM, Turyshev SG. Indication, from Pioneer 10/11, Galileo, and Ulysses data, of an apparent anomalous, weak, long-range acceleration. Physical Review Letters. 1998;**81**:2858-2861

[57] Turyshev SG, Toth VT, Kellogg LR, Lau EL, Lee KJ. A study of the Pioneer anomaly: New data and objectives for new investigation. International Journal of Modern Physics D. 2006;**15**(01):1-55

[58] Iorio L. Can the pioneer anomaly be of gravitational origin? A phenomenological answer. Foundations of Physics. 2007;**37**:897-918

[59] Anderson JD, Laing PA, Lau EL, Liu AS, Nieto MM, Turyshev SG. Study of the anomalous acceleration of Pioneer 10 and 11. Physical Review D. 2002;**65**: 082004

[60] Turyshev SG, Toth VT, Kinsella G, Lee S-C, Lok SM, Ellis J. Support for the thermal origin of the Pioneer anomaly. Physical Review Letters. 2012;**108**: 241101

[61] Wilhelm K, Dwivedi BN. An explanation of the pioneer anomaly in the framework of a gravitational impact model. Astrophysics and Space Sciences Transactions. 2011;**7**:487-494

[62] Lämmerzahl C, Preuss O, Dittus H. Is the physics within the solar system really understood? In: Dittus H, Lämmerzahl C, Turyshev SG, editors. Lasers, Clocks and Drag-free Control: Exploration of Relativistic Gravity in

Space. Vol. 349. Astrophysics and Space Science Library; 2008. pp. 75-101

[63] Wilhelm K, Dwivedi BN. Increase of the mean Sun-Earth distance caused by a secular mass accumulation. Astrophysics and Space Science. 2013; **347**:41-45

[64] Bureau International des Poids et Mesures, Le Système International d'Unités (SI), 8e éd. Sèvres: BIPM; 2014

[65] Pitjeva EV, Standish EM. Proposals for the masses of the three largest asteroids, the Moon-Earth mass ratio and the astronomical unit. Celestial Mechanics and Dynamical Astronomy. 2009;**103**:365-372

[66] Anderson JD, Nieto MM. Astrometric solar-system anomalies. Relativity in fundamental astronomy: Dynamics, reference frames, and data analysis. Proceedings of the International Astronomical Union, IAU Symposium. 2010;**261**:189-197

[67] Harmanec P, Prša A. The call to adopt a nominal set of astrophysical parameters and constants to improve the accuracy of fundamental physical properties of stars. PASP. 2011;**123**: 976-980

[68] Wilhelm K, Dwivedi BN. Secular perihelion advances of the inner planets and asteroid Icarus. New Astronomy. 2014;**31**:51-55

[69] Anderson JD, Campbell JK, Ekelund JE, Ellis J, Jordan JF. Anomalous orbital-energy changes observed during spacecraft flybys of Earth. Physical Review Letters. 2008; **100**:091102

[70] Nieto MM, Anderson JD. Earth flyby anomalies. Physics Today. 2009; **62**:76-77

[71] Acedo L. The flyby anomaly: A multivariate analysis approach. Astrophysics and Space Science. 2017; **362**:42

[72] Wilhelm K, Dwivedi BN. Anomalous Earth flybys of spacecraft. Astrophysics and Space Science. 2015; **358**:18

[73] Landau LD, Lifshitz EM. Course of Theoretical Physics. Vol. 1. Mechanics. 3rd ed. Oxford, New York, Toronto, Sydney, Paris, Frankfurt: Pergamon Press; 1976

[74] Acedo L, Piqueras P, Moraño JA. A possible flyby anomaly for Juno at Jupiter. Advances in Space Research. 2018;**61**:2697-2706

[75] Wilhelm K, Dwivedi BN. Impact models of gravitational and electrostatic forces: Potential energies, atomic clocks, gravitational anomalies and redshift. arXiv: 1804.04010. 2018 [Accessed: 30 October 2019]

[76] Rubin VC. Dark matter in spiral galaxies. Scientific American. 1983;**248**: 96-106

[77] Rubin VC. Dark matter in the Universe. Highlights of Astronomy. 1986;**7**:27-38

[78] Oort JH. The force exerted by the stellar system in the direction perpendicular to the galactic plane and some related problems. Bulletin of the Astronomical Institutes of the Netherlands. 1932;**6**:249-287

[79] Zwicky F. Die Rotverschiebung von extragalaktischen Nebeln. Helvetica Physica Acta. 1933;**6**:110-127

[80] Milgrom M. A modification of the Newtonian dynamics as a possible alternative to the hidden mass hypothesis. Astrophysical Journal. 1983; **270**:365-370

[81] Wilhelm K, Dwivedi BN. A physical process of the radial acceleration of disc

galaxies. Monthly Notices of the Royal Astronomical Society. 2018;**474**: 4723-4729

[82] McGaugh SS, Lelli F, Schombert JM. Radial acceleration relation in rotationally supported galaxies. Physical Review Letters. 2016;**117**:201101

[83] McGaugh SS. Balance of dark and luminous mass in rotating galaxies. Physical Review Letters. 2005;**95**:171302

[84] Fraternali F, Sancisi R, Kamphuis P. A tale of two galaxies: Light and mass in NGC 891 and NGC 7814. Astronomy & Astrophysics. 2011;**531**:A64

[85] Salucci P, Turini N Evidences for collisional dark matter in galaxies? arXiv: 1707.01059. 2017 [Accessed: 26 October 2019]

[86] Soldner J. Ueber die Ablenkung eines Lichtstrals von seiner geradlinigen Bewegung durch die Attraktion eines Weltkörpers, an welchem er nahe vorbei geht. Berliner Astronomisches Jahrbuch. 1804;**1804**:161-172

[87] Einstein A. Über den Einfluß der Schwerkraft auf die Ausbreitung des Lichtes. Annalen der Physik (Leipzig). 1911;**340**:898-908

[88] Schiff LI. On experimental tests of the general theory of relativity. American Journal of Physics. 1960;**28**: 340-343

[89] Dyson FW, Eddington AS, Davidson C. A determination of the deflection of light by the Sun's gravitational field, from observations made at the total eclipse of May 29, 1919. Philosophical Transactions of the Royal Society of London A. 1920;**220**: 291-333

[90] Mikhailov AA. The deflection of light by the gravitational field of the Sun. Monthly Notices of the Royal Astronomical Society. 1959;**119**:593-608

[91] Wilhelm K, Dwivedi BN. Gravity, massive particles, photons and Shapiro delay. Astrophysics and Space Science. 2013;**343**:145-151

[92] Goldhaber AS, Nieto MM. Terrestrial and extraterrestrial limits on the photon mass. Reviews of Modern Physics. 1971;**43**:277-296

[93] Amsler C, Doser M, Antonelli M, et al. Review of particle physics. Physics Letters B. 2008;**667**:1-1340

[94] Yang Y-P, Zhang B. Tight constraint on photon mass from pulsar spindown. Astrophysical Journal. 2017;**842**:23

[95] Wilhelm K, Dwivedi BN. Gravitational redshift and the vacuum index of refraction. Astrophysics and Space Science. 2019;**364**(2)id.26

[96] Wilhelm K, Dwivedi BN. On the gravitational redshift. New Astronomy. 2014;**31**:8-13

[97] Fermi E. Quantum theory of radiation. Reviews of Modern Physics. 1932;**4**:87-132

[98] Sommerfeld A. Optik. Verlag Harri Deutsch: Thun, Frankfurt/Main; 1978

[99] Boonserm P, Cattoen C, Faber T, Visser M, Weinfurtner S. Effective refractive index tensor for weak-field gravity. Classical and Quantum Gravity. 2005;**22**:1905-1916

[100] Ye X-H, Lin Q. Gravitational lensing analysed by the graded refractive index of a vacuum. Journal of Optics A: Pure and Applied Optics. 2008;**10**(7):075001

[101] Okun LB. Photons and static gravity. Modern Physics Letters A. 2000;**15**:1941-1947

[102] Shapiro II. Fourth test of general relativity. Physical Review Letters. 1964;**13**:789-791

[103] Reasenberg RD, Shapiro II, MacNeil PE, Goldstein RB, Breidenthal JC, Brenkle JP, et al. Viking relativity experiment: Verification of signal retardation by solar gravity. Astrophysical Journal. 1979;**234**:L219-L221

[104] Shapiro II, Ash ME, Ingalls RP, Smith WB, Campbell DB, Dyce RB, et al. Fourth test of general relativity: New radar result. Physical Review Letters. 1971;**26**:1132-1135

[105] Kramer M, Stairs IH, Manchester RN, et al. Tests of general relativity from timing the double pulsar. Science. 2006;**314**:97-102

[106] Ballmer S, Márka S, Shawhan P. Feasibility of measuring the Shapiro time delay over meter-scaled distances. Classical and Quantum Gravity. 2010; **27**:185018-185011

[107] Kutschera M, Zajiczek W. Shapiro effect for relativistic particles—Testing general relativity in a new window. Acta Physica Polonica B. 2010;**41**:1237-1246

[108] Einstein A. Lichtgeschwindigkeit und Statik des Gravitationsfeldes. Annalen der Physik (Leipzig). 1912;**343**: 355-369

[109] Einstein A. Über das Relativitätsprinzip und die aus demselben gezogenen Folgerungen. Jahrbuch der Radioaktivität und Elektronik. 1907;**1908**(4):411-462

[110] Kollatschny W. AGN black hole mass derived from the gravitational redshift in optical lines

[111] Negi PS. An upper bound on the energy of a gravitationally redshifted electron-positron annihilation line from the Crab pulsar. Astronomy & Astrophysics. 2005;**431**:673-677

[112] Lämmerzahl C. What determines the nature of gravity? A phenomenological approach. Space Science Reviews. 2009;**148**:501-522

[113] Pasquini L, Melo C, Chavero C, Dravins D, Ludwig H-G, Bonifacio P, et al. Gravitational redshifts in main-sequence and giant stars. Astronomy & Astrophysics. 2011;**526**:A127

[114] Turyshev SG. Testing fundamental gravitation in space. Nuclear Physics B (Proceedings Supplement). 2013;**243**: 197-202

[115] Will CM. Gravitational red-shift measurements as tests of nonmetric theories of gravity. Physical Review D. 1974;**10**:2330-2337

[116] Okun LB, Selivanov KG, Telegdi VL. On the interpretation of the redshift in a static gravitational field. American Journal of Physics. 2000;**68**: 115-119

[117] Sinha S, Samuel J. Atom interferometry and the gravitational redshift. Classical and Quantum Gravity. 2011;**28**:145018-1-145018-8

[118] Pound RV, Rebka GA. Gravitational red-shift in nuclear resonance. Physical Review Letters. 1959;**3**:439-441

[119] Krause IY, Lüders G. Experimentelle Prüfung der Relativitätstheorie mit Kernresonanzabsorption. Naturwissenschaften. 1961;**48**:34-36

[120] Pound RV, Snider JL. Effect of gravity on gamma radiation. Physical Review. 1965;**140**:788-803

[121] Vessot RFC, Levine MW, Mattison EM, Blomberg EL, Hoffman TE, Nystrom GU, et al. Test of relativistic gravitation with a space-borne hydrogen maser. Physical Review Letters. 1980;**45**:2081-2084

[122] LoPresto JC, Schrader C, Pierce AK. Solar gravitational redshift from the

infrared oxygen triplet. Astrophysical Journal. 1991;**376**:757-760

[123] Takeda Y, Ueno S. Detection of gravitational redshift on the solar disk by using iodine-cell technique. Solar Physics. 2012;**281**:551-575

[124] Mannheim PD. Alternatives to dark matter and dark energy. Progress in Particle and Nuclear Physics. 2006; **56**:340-445

[125] Sotiriou TP, Liberati S, Faraoni V. Theory of gravitation theories: A no-progress report. International Journal of Modern Physics D. 2008;**17**:399-423

[126] Scott RB. Teaching the gravitational redshift: Lessons from the history and philosophy of physics. Journal of Physics: Conference Series. 2015;**600**:012055

[127] Møller C. On the possibility of terrestrial tests of the general theory of relativity. Nuovo Cimento. 1957;**6**: 381-398

[128] Cranshaw TE, Schiffer JP, Whitehead AB. Measurement of the gravitational red shift using the Mössbauer effect in Fe^{57}. Physical Review Letters. 1960;**4**:163-164

[129] Ohanian HC. Gravitation and Spacetime. New York: W.W. Norton; 1976

[130] Hay HJ, Schiffer JP, Cranshaw TE, Egelstaff PA. Measurement of the red shift in an accelerated system using the Mössbauer effect in Fe^{57}. Physical Review Letters. 1960;**4**:165-166

[131] Straumann N. General Relativity with Applications to Astrophysics. Berlin, Heidelberg, New York: Springer-Verlag; 2004

[132] Randall L. Verborgene Universen. 4. Auflage. Frankfurt/Main: S. Fischer Verlag GmbH; 2006

[133] Will CM. The confrontation between general relativity and experiment. Living Reviews in Relativity. 2014;**17**(4):1-117 [Accessed: 27 October 2019]

[134] Pound RV. Weighing photons. Classical and Quantum Gravity. 2000; **17**:2303-2311

[135] Michelson AA, Morley EW. On the relative motion of the Earth and of the luminiferous ether. Sidereal Messenger. 1887;**6**:306-310

[136] Wiechert E. Relativitätsprinzip und Äther. Physikalische Zeitschrift. 1911;**12**: 689-707, 737-758

[137] Schröder W. Ein Beitrag zur frühen Diskussion um den Äther und die Einsteinsche Relativitätstheorie. Annalen der Physik. 1990;**502**:475-489

[138] von Laue M. Zwei Einwände gegen die Relativitätstheorie und ihre Widerlegung. Physikalische Zeitschrift. 1912;**XIII**:118-120

[139] von Laue M. Geschichte der Physik. 4. erweiterte. Auflage. Ullstein Taschenbücher-Verlag: Frankfurt/Main; 1959

[140] Einstein A. Äther und Relativitätstheorie, Rede gehalten am 5. Mai 1920 an der Reichs-Universität zu Leiden. Berlin: Verlag von Julius Springer; 1920

[141] Einstein A. Über den Äther. Verhandlungen der Schweizerischen Naturforschenden. Gesellschaft. 1924; **105**:85-93

[142] Michelson AA, Lorentz HA, Miller DC, Kennedy RJ, Hedrick ER, Epstein PS. Conference on the Michelson-Morley experiment held at Mount Wilson, February, 1927. Astrophysical Journal. 1928;**68**:341-402

[143] Dirac PAM. Is there an æther? Nature. 1951;**168**:906-907

[144] Granek G. Einstein's ether: F. Why did Einstein come back to the ether? Apeiron. 2001;**8**:19-28

[145] Dirac PAM. The quantum theory of the emission and absorption of radiation. Proceedings of the Royal Society of London. Series A. 1927;**114**: 243-265

[146] Vigier JP. Explicit mathematical construction of relativistic nonlinear de Broglie waves described by three-dimensional (wave and electromagnetic) solitons "piloted" (controlled) by corresponding solutions of associated linear Klein-Gordon and Schrödinger equations. Foundations of Physics. 1991;**21**:125-148

[147] Kamenov P, Slavov B. The photon as a soliton. Foundations of Physics Letters. 1998;**11**:325-342

[148] Meulenberg A. The photonic soliton. SPIE Conference Proceedings. 2013;**8832**:88320M

[149] Bersons I. Soliton model of the photon. Latvian Journal of Physics and Technical Sciences. 2013;**50**:60-67

[150] Bertotti B, Iess L, Tortora P. A test of general relativity using radio links with the Cassini spacecraft. New Astronomy. 2003;**425**:374-376

[151] Ellis RS. Gravitational lensing: A unique probe of dark matter and dark energy. Philosophical Transactions of The Royal Society A: Mathematical, Physical and Engineering Sciences. 2010;**368**:967-987

[152] Hildebrandt H, Viola M, Heymans C, Joudaki S, Kuijken K, the KIDS collaboration. KiDS-450: Cosmological parameter constraints from tomographic weak gravitational lensing. Monthly Notices of the Royal Astronomical Society. 2017;**465**: 1454-1498